Incorporation of the Influences of Kinematics Parameters and Joints Tilting for the Calibration of Serial Robotic Manipulators

DHAVALKUMAR ARUNBHAI PATEL

School of Mechanical Engineering

University of Adelaide

Submitted to the Graduate Centre of University of Adelaide for the degree of

Master of Philosophy

(Mechanical Engineering)

December 2017

DECLARATION

I certify that this work contains no material which has been accepted for the award of any other degree or diploma in my name, in any university or other tertiary institution and, to the best of my knowledge and belief, contains no material previously published or written by another person, except where due reference has been made in the text. In addition, I certify that no part of this work will, in the future, be used in a submission in my name, for any other degree or diploma in any university or other tertiary institution without the prior approval of the University of Adelaide and where applicable, any partner institution responsible for the joint-award of this degree.

I give consent to this copy of my thesis when deposited in the University Library, being made available for loan and photocopying, subject to the provisions of the Copyright Act 1968.

I acknowledge that copyright of published works / submitted for publication contained within this thesis resides with the copyright holder(s) of those works.

I also give permission for the digital version of my thesis to be made available on the web, via the University's digital research repository, the Library Search and also through web search engines, unless permission has been granted by the University to restrict access for a period of time.

Name: Dhavalkumar Arunbhai Patel

Signature:

Date: 13 Feb 2018

Table of Contents

LIST OF FIGURES

LIST TABLES

LIST OF NOMENCLATURES

α_i	Joint twist angle about X- axis
β_i	Joint twist angle about Y- axis
θ_i	Joint angle about Z- axis
a_i	Link length
d_i	Link offset
${}^{i-1}_{i}T$	Transformation between the frames $\{i-1\}$ and $\{i\}$
X	Robot end-effector coordinate
Y	Robot end-effector coordinate
Z	Robot end-effector coordinate
φ	Robot end-effector orientation angle
θ	Robot end-effector orientation angle
Ψ	Robot end-effector orientation angle
P	Robot end-effector pose vector
ΔP	Robot end-effector pose error vector
J	Jacobin
η_i	Vector of moments about joint i
F_i	Vector of forces acting at frames $\{i\}$
$C_i^{cle\ tilt}$	Joint inclination angle
r_i^{cle}	Joint clearance
γ_i	Angle of contact point
Δ	Geometric joint error prefix
δ	Non-geometric joint error prefix

LIST OF ABBREVIATIONS

POSE	Position and orientation
DH	Denavit Hartenberg
MDH	Modified Denavit Hartenberg
IDH	Improved Denavit Hartenberg
CPC	Complete and Parametrically Continuous
MCPC	Modified Complete and Parametrically Continuous
POE	Product of Exponentials
IMU	Inertial Measurement Unit
PSD	Position Sensitive Device
CMM	Coordinate Measuring Machine
MLCS	Model-based on Local-link Coordinate System
MGSC	Model-based on Global Coordinate System
CCD	Charge-Coupled Device
TCP	Tool Centre Point
AI	Artificial Intelligence
KF	Kalman Filter
EKF	Extended Kalman Filter
DOF	Degree of Freedom
CEPs	Calibrated Error Parameters
RBFN	Radial Basis Function Network
ANN	Artificial Neural Network
CPA	Circle Point Analysis
CAD	Computer Aided Design
OLP	Off-line Programming

ABSTRACT

Serial robotic manipulators are calibrated to improve and restore their accuracy and repeatability. Kinematics parameters calibration of a robot reduces difference between the model of a robot in the controller and its actual mechanism to improve accuracy. Kinematics parameter's error identification in the standard kinematics calibration has been configuration independent which does not consider the influence of kinematics parameter on robot tool pose accuracy for a given configuration. This research analyses the configuration dependent influences of kinematics parameters error on pose accuracy of a robot. Based on the effect of kinematics parameters, errors in the kinematics parameters are identified. Another issue is that current kinematics calibration models do not incorporate the joints tilting as a result of joint clearance, backlash, and flexibility, which is critical to the accuracy of serial robotic manipulators, and therefore compromises a pose accuracy. To address this issue which has not been carefully considered in the literature, this research suggested an approach to model configuration dependent joint tilting and presents a novel approach to encapsulate them in the calibration of serial robotic manipulators. The joint tilting along with the kinematics errors are identified and compensated in the kinematics model of the robot. Both conventional and proposed calibration approach are tested experimentally, and the calibration results are investigated to demonstrate the effectiveness of this research. Finally, the improvement in the trajectory tracking accuracy of the robot has been validated with the help of proposed low-cost measurement set-up.

PUBLICATIONS

Accepted

Conference paper

Patel, D., T.-F. Lu, and L. Chen, An Influence Based Error Identification for Kinematics Calibration of Serial Robotic Manipulators, *in 5th IFToMM International Symposium on Robotics & Mechatronics (ISRM2017)*. 2017: Sydney, Australia.

Under review

Journal paper 1

PATEL, D., LU, T.-F. & CHEN, L. 2017. Investigation of Influence of Joints Tilting for Calibration of Serial Robotic Manipulators. *International Journal of Precision Engineering and Manufacturing.*

Journal paper 2

PATEL, D., LU, T.-F. & CHEN, L. 2017. Calibration of serial robots to improve trajectory tracking accuracy by considering joints tilting using a low-cost measurement method. *Robotica.*

ACKNOWLEDGEMENT

I would like to begin by thanking my supervisors Dr Tien-Fu Lu and Dr Lei Chen for their advice, guidance, encouragement, and support throughout the candidature. They also provided the perfect research area to work with, which encapsulates both theoretical and practical components of the robotics field. Also, my friends and colleagues at the school of mechanical engineering, they shared their knowledge and experience on the courses and the work that they have done, but more importantly they made my university career a lot more interesting. I would like to thank School of Mechanical Engineering, the University of Adelaide for providing me with a life-changing experience. Finally, I would like to thank my wife, my son, and my parents for their constant support in all aspects.

CHAPTER 1 INTRODUCTION

1.1 Motivation

Serial robotic manipulators are extensively used in manufacturing, medical, automobile assembly lines, outer space, and so forth. Serial manipulators have superior repeatability compared to their accuracy. Repeatability is the ability of the manipulator to return to the same pose (i.e. position and orientation) from the same direction. Multidirectional repeatability can be even worse than unidirectional repeatability. Whereas, accuracy is the ability of the robot to attain a commanding pose on a fixed reference frame (generally, robots base). Repeatability of current serial robots is roughly 0.05 mm (To, 2012). However, an absolute accuracy usually is not documented by robot manufacturers which vary from 10mm to a few millimetres for industrial robots. The requirement for industrial robots having better pose (i.e. position and orientation) accuracy has continuously been increasing in the past decade. Due to the serial connection of the links, end-effector of a serial robot can follow complex profile and reach into the congested places. Therefore, the serial robots have growing numbers of application especially in the automobile manufacturing, medical sector such as laser cutting of stamped steel using serial robotic manipulators, remote surgery and so on. Moreover, in off-line programming (OLP), the accuracy becomes an essential issue since programmer virtually defines the positions from an absolute or relative coordinate system. For example, during the assembly process of the Airbus A340 wing panels, approximately 65,000 holes must be drilled on each skin. The tolerance for a drilled hole in aerostructure assembly is usually 0.2 mm (To, 2012). In such scenarios, manual compensation of robot inaccuracy is costly, time-consuming or even impossible in some cases. Therefore, gives the motivation for the research on the calibration of serial robotic manipulators to improve their accuracy.

1.2 Robot Calibration Background

Serial robotic manipulators are made of serially connected links by joints. Pose accuracy of serial robots is affected by various geometric factors such as an error in links' length, joints' orientation, and encoders offset as well as non-geometric factors such as joint clearance, backlash, joints flexibility (i.e. joint compliance), dynamic

parameters, friction, and links deformation (Shiakolas et al., 2002). The other factors that have a tiny effect on the pose accuracy of serial robots are temperature, humidity, installation errors, electrical noise, measurement resolution, non-linearity of the encoder, calculation process and control error. The geometric parameters errors can be systematically identified and compensated whereas other errors are difficult to model and identify. All these factors introduce the difference between the model of the robot on the controller and its actual mechanism as shown in Fig. 1.1. Therefore, calibration has been carried out to minimise this difference to improve the accuracy of serial robotic manipulators.

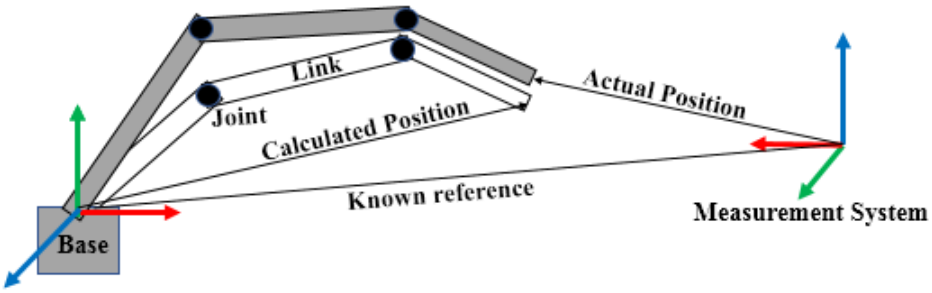

Fig. 1.1 Pose error

Following the large numbers of factors affecting the pose accuracy of serial robotic manipulators, there are three different level of calibrations carried out in practise (Mooring et al., 1991). The level 1 calibration is to correct robot's joint encoder's reading with the help of end-effectors pose measurement. The level 1 calibration is also known as zero offset calibration where kinematics parameters are not modified, but only joint encoders' offsets are corrected. The level 2 calibration additionally modifies the kinematic parameters (i.e. geometric parameters such as joint twist and link length) in the robot controller to achieve better pose accuracy. The level 3 calibration incorporates modification of geometric parameters as well as non-geometric parameters affecting the pose accuracy, which is extremely complicated to perform.

The main reason that causes the pose error is inaccurate geometric parameters used to calculate the pose. Experimental results reported by (Renders et al., 1991) conclude that geometric errors can be as much as 90 % responsible for robot pose errors. So often level 2 calibration fulfils the desired pose accuracy for many applications. Level 2 calibration is also known as the kinematics calibration. In this calibration process, the kinematics parameters are modified such as to minimize the difference between

the kinematics model of the robot in the controller and the actual mechanism of the robot. Robot kinematics calibration includes four steps (Mooring et al., 1991), namely kinematics and error modelling, end-effector pose measurement, identification of error sources and compensation of the errors into the kinematic model as shown in Fig. 1.2.

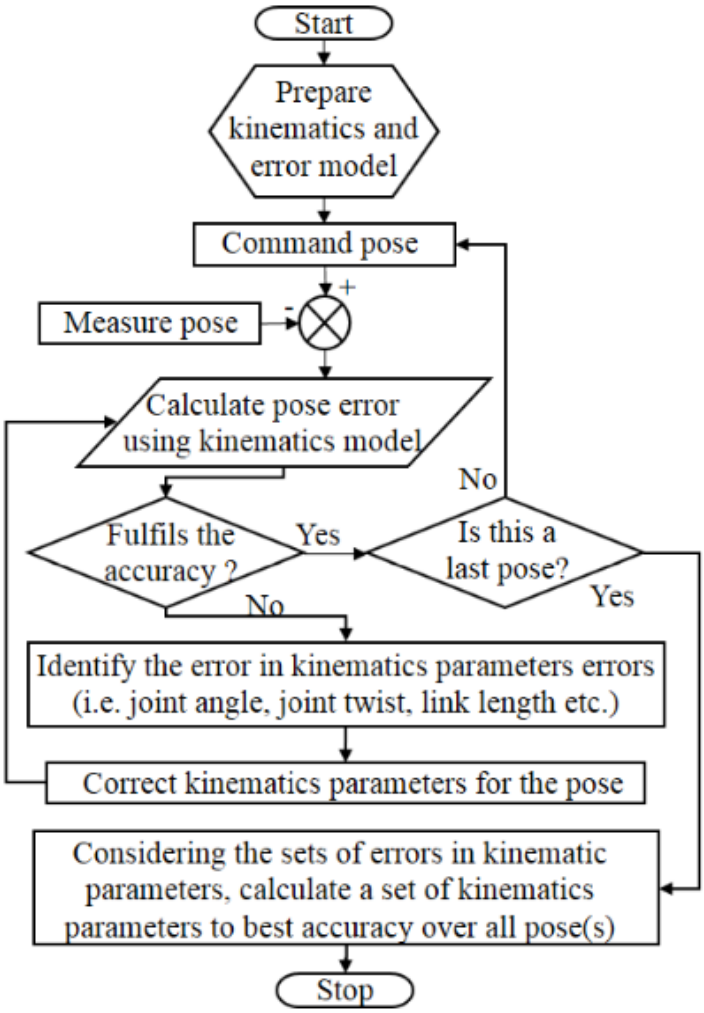

Fig. 1.2 Standard kinematics calibration process

Calibration is also considered as an absolute calibration and relative calibration. An absolute calibration considers the robot base whereas a relative calibration disregards the actual location of the robot base. If we want more than one robot to share the same coordinate or to be programmed off-line, needs the robot to be absolute calibrated. For the absolute calibration, measurement systems such as a laser tracker, cameras, and CMM are used to directly measure the pose of a robot tool. A relative calibration is of interest when we are positioning the robot relative to a local frame, so we need a tool, such as a touch probe, which allows us to locate objects in the robot working space. When the robot is placed at the contact position, the joint values given

by the encoders are registered. An absolute calibration needs six more parameters than a relative calibration because we need to represent the relative frame on an absolute frame.

1.3 Research purpose

Conventionally identified errors in the kinematics parameters of a robot are only approximated set of kinematics parameters errors that can best fit the difference between the actual and the nominal value of end-effectors pose (Chen-Gang et al., 2014). Errors identification does not account for the influence of kinematics parameters as a given pose. Hence, compensation for constant kinematics parameters' errors cannot guarantee the improvement in the pose accuracy at all the points in the workspace. The improvement in the pose accuracy remains limited up to few calibrated points or the small region of the workspace. Pose accuracy at some points in the workspace may become worse after the calibration due to the constant error compensation. (Zhou et al., 2014, Tao et al., 2012, Jang et al., 2001) considered joints flexibility in addition to the geometric parameters during the calibration. (Zhou et al., 2014) suggested that non-geometric factors such as joints flexibility can affect the pose accuracy of a robot up to 37%, and hence must be considered during robot calibration. Moreover, kinematics calibration models used in the present calibration process does not incorporate all joint parameters. For example, present calibration models do not consider joints tilting due to combined effect of joint clearance, backlash, and flexibility. Additionally, large volume metrology equipment such as Laser tracker and Optical CMM increase the cost of robot calibration (Wang et al., 2012).

Therefore, the aim of this project is to consider influence of kinematics parameters during geometric errors identification, and incorporate joints tilting which is the combined effect of non-geometric parameters in robot calibration. Also, to find a low-cost measurement alternative to costly measurement equipment for the validation of improvement in the accuracy of a robot after the calibration.

1.4 Thesis synopsis

The content of this thesis is divided into five sections. The first section reviews existing kinematics models, measurement methods, errors identification and compensation techniques employed in the contemporary robot calibration process (Chapter 2). The second section proposes influence based error identification (Chapter 3). The third section model and analyses effect of joints tilting (Chapter 4). The fourth section implements proposed joint tilting model to improve trajectory tracking accuracy using low-cost measurement set-up (Chapter 5). The last section discusses the contribution of this research and directions for the future scope of work. Details of each chapter are as follows.

Chapter 2: This chapter reviews the previous research conducted on the serial robot calibration to find difficulties associated with the calibration process. Robot calibration models, measurement techniques, and errors identification are the focus of the literature review and given attention to finding a scope of research.

Chapter 3: This chapter analyses configuration dependent effect of kinematics parameters error on the pose accuracy of a serial robot. The chapter also redefines the conventional kinematics error detection by introducing influence based error identification.

Chapter 4: This chapter proposes a mathematics required to incorporate joints tilting under the effect of joints clearance, backlash, and joints flexibility. Joints clearance, stiffness and backlash are measured directly. The proposed method to incorporate joints tilting in robot calibration is validated experimentally by following the ISO 9283 guidelines for the assessment of robot accuracy.

Chapter 5: This chapter combinedly applies robot dynamics and joint tilting model to improve trajectory tracking accuracy of the Katana robot, and validates improvement in the tracking accuracy with a low-cost measurement set-up.

Chapter 6: This chapter summarises this research and present a future work.

CHAPTER 2 LITERATURE REVIEW

Considering the process of calibration, the literature review is divided into four parts. The first segment of the literature review focuses on the existing kinematics modelling methods used for the calibration of serial robotic manipulators. The second part of the literature discusses the measurement technologies available to use for the calibration of the serial robotic manipulators, the third segment thoroughly reviews methods used for geometric and non-geometric parameters error identification, and the fourth section discusses errors compensation. The chapter end would summarise the literature, highlights research gaps, and establishes aims and objectives of this research.

2.1 Kinematics and error modelling

Kinematics model of a robot establishes relationship between the robot's joint-link parameters (shown in Fig. 2.1) and the pose (i.e. position and orientation) of robot end-effector. The kinematics model of the manipulators must be complete (i.e. sufficient parameters to describe the robot's kinematics), continuous, non-redundant (i.e. use of a minimum number of kinematics parameters) and feasible for the calibration. Chen-Gang et al. (2014) summarised various methods of kinematics modeling for manipulators such as DH (Denavit-Hartenberg) method, modified DH method, improved DH method, CPC (complete and parametrically continuous) method and MCPC (modified CPC) method. All these methods have been evolved from DH method, and either uses more parameters or different combinations of parameters.

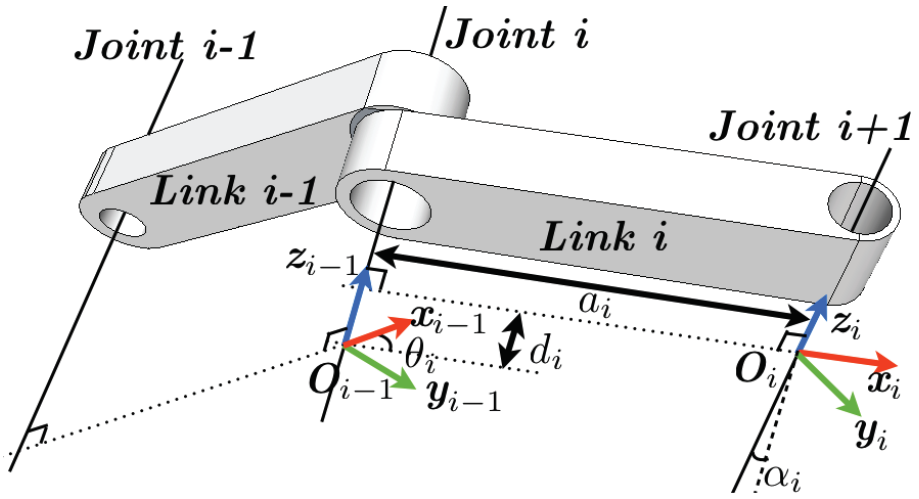

Fig. 2.1 Original DH method

The Original DH method uses two linear parameters d_i and a_i, and two rotational parameters θ_i to α_i to correlate two links (i.e. frames) shown in Fig. 2.1. The homogeneous link transformation matrix ${}^{i-1}_{i}T$ is formed by multiplying four transformations as:

$$ {}^{i-1}_{i}T = Trans(Z, d_i)Rot(Z, \theta_i)Trans(X, a_i)Rot(X, \alpha_i) \tag{2.1} $$

So, for the n-DOF serial robot, a kinematics model derived using the DH method requires 4r+2p+6 geometric parameters, where r and p represents revolute and prismatic joints respectively. For universal six DOF robot, the relationship between base frame and tool (end-effector) of the robot can be derived by multiplying all the transformation metrics as:

$$ {}^{Base}_{Tool}T = {}^{Base}_{1}T \cdot {}^{1}_{2}T \cdot {}^{2}_{3}T \cdot {}^{3}_{4}T \cdot {}^{4}_{5}T \cdot {}^{5}_{6}T \cdot {}^{6}_{Tool}T \tag{2.2} $$

$$ {}^{Base}_{Tool}T = \begin{bmatrix} R_{11} & R_{12} & R_{13} & X \\ R_{21} & R_{22} & R_{23} & Y \\ R_{31} & R_{32} & R_{33} & Z \\ 0 & 0 & 0 & 1 \end{bmatrix} \tag{2.3} $$

Equation (2.2) is called forward kinematics model of the robot. The robot end-effector pose can be described as $P = [X \;\; Y \;\; Z \; \Phi \; \theta \; \Psi]^T$. The positional parameters X, Y and Z of the end-effector vector P can be obtained directly from (2.3). However, a set of Euler angles method (i.e. ZXZ, ZYZ etc.) or fixed angles method must be used to decompose rotational parameters from (2.3) in the form of orientation angles Φ, θ and Ψ. For example, ZXZ Euler angles method employed in this research defines $\Phi = \tan^{-1}(R_{13}/-R_{23})$, $\theta = \tan^{-1}((-R_{23}\cos\Phi + R_{13}\sin\Phi)/R_{33})$, and $\Psi = \tan^{-1}(R_{31}/R_{32})$. In the DH method, the coordinate system and parameters are defined strictly, and hence kinematics models are consistent. The DH method used to be the standard method for robot kinematics modeling and employed widely.

However, due to the constraint imposed on the base coordinate system, the orientation of the base coordinate system is related to the first joint, which restricts the arbitrary assignment of base coordinates. Craig (1990) introduced the modified DH method by adding transformation at joint as in (2.4) to overcome the issue, where robot's base

$$ {}^{i-1}_{i}T = Rot(X, \alpha_{i-1})Trans(X, a_{i-1})Rot(Z, \theta_i)Trans(Z, d_i) \tag{2.4} $$

coordinate system and first joint parameters are not related. However, in both models

when the adjacent joint axes are parallel, the small tilt may cause the dramatic parameters to change that can lead to the discontinuity.

Hayati and Mirmirani (1985) suggested the use of an additional parameter β as in (2.5) to avoid discontinuity when two consecutive joint axes are parallel. However,

$$^{i-1}_{i}T = Rot(Z,\theta_i)Trans(Z,d_i)Rot(X,\alpha_i)Trans(X,\beta_i) \tag{2.5}$$

arbitrary assignment of base and tool coordinate is not possible in the original, modified or the improved DH method. Moreover, all the DH methods are incomplete as it is not possible to identify all kinematics errors with four joint link parameters (i.e. two translational and two rotational parameters) and thus cannot compensate all the errors during the calibration. Aiming at the incompleteness of the kinematics model, the S-model added two extra parameters to the DH model and used six parameters to allow an arbitrary placement of the link frames (Chen-Gang et al., 2014). The S-model is complete but not parametrically continuous. Zhuang et al. (1990) introduced the CPC model to facilitates arbitrary assignment of base and tool frame. The relationship between the links is defined with three translations and one rotation parameters instead of two translations and two rotations. The CPC model is complete and parametrically continuous. The error model in the CPC model is singularity-free but requires additional condition handling. The additional parameters handling makes the modeling task unnecessarily complex. Zhuang et al. (1993) uses three rotational and two linear parameters to simplify the modeling task, which is close to the DH method. However, the error model becomes singular if the tool axis is perpendicular to the last joint axis.

The other model such as the Product of Exponentials (POE) uses the general spatial rigid body displacement equation (i.e. screw coordinate system in the global coordinate system) with six parameters (Park and Okamura, 1994). Due to the modelling complexity, the models based on global coordinate system (i.e. such as POE and zero referenced model) are not used widely for the kinematics calibration. Kinematics modelling using MCPC model and POE based model gives a complete and continuous model with added complexity (Chen-Gang et al., 2014).

Following the kinematics model, the error model is established to incorporate the kinematics parameters errors once identified. The error model must be able to correlate the pose errors of robot's end-effector with the kinematics parameters errors. Considering the errors of kinematics parameters, the pose error ΔP between the actual pose P_a and the theoretical pose P_t of the end-effectors can be described as:

$$\Delta P = P_a - P_t = [\Delta X \;\; \Delta Y \;\; \Delta Z \; \Delta \Phi \; \Delta \theta \;\; \Delta \Psi]^T \tag{2.6}$$

If ${}^{i-1}_{i}T^a$ and ${}^{i-1}_{i}T^t$ represent the actual and nominal transformation from the $(i-1)^{th}$ to the i^{th} coordinate systems respectively, the deviation of transformation matrix ${}^{i-1}_{i}dT$ for the adjacent link coordinate systems can be expressed in the form of the kinematics parameters $Q_{i,j}$, and the errors of kinematics parameters $\Delta Q_{i,j}$ in that transformation matrix as:

$${}^{i-1}_{i}dT = {}^{i-1}_{i}T^a - {}^{i-1}_{i}T^t = \sum_{j=1}^{6} \frac{\partial T_i^t}{\partial Q_{i,j}} \Delta Q_{i,j}. \tag{2.7}$$

If s is the number of kinematics parameters in each transformation, and i is total number of links. The deviation of the end-effectors pose ΔP in (2.6) can be represented by combining partial derivative in (2.7) for all links (Ha, 2008). Therefore, by differentiating the kinematics equation, we can obtain deviation of end-effectors pose as:

$$\Delta P = \sum_{i=1}^{6} \sum_{j=1}^{s} \frac{\partial P}{\partial Q_{i,j}} \Delta Q_{i,j} \tag{2.8}$$

The pose errors vector ΔP can be correlated to the kinematics parameters error vector ΔE with the help of the mapping matrix J as:

$$\Delta P = J.\Delta E. \tag{2.9}$$

Where, $J = \begin{bmatrix} \frac{\partial P_X}{\partial \theta_1} .. \frac{\partial P_X}{\partial \theta_5} & \frac{\partial P_X}{\partial \alpha_0} .. \frac{\partial P_X}{\partial \alpha_5} & \frac{\partial P_X}{\partial a_0} .. \frac{\partial P_X}{\partial a_5} & \frac{\partial P_X}{\partial d_1} .. \frac{\partial P_X}{\partial d_6} \\ \frac{\partial P_Y}{\partial \theta_1} .. \frac{\partial P_Y}{\partial \theta_5} & \frac{\partial P_Y}{\partial \alpha_0} .. \frac{\partial P_Y}{\partial \alpha_5} & \frac{\partial P_Y}{\partial a_0} .. \frac{\partial P_Y}{\partial a_5} & \frac{\partial P_Y}{\partial d_1} .. \frac{\partial P_Y}{\partial d_6} \\ \frac{\partial P_Z}{\partial \theta_1} .. \frac{\partial P_Z}{\partial \theta_5} & \frac{\partial P_Z}{\partial \alpha_0} .. \frac{\partial P_Z}{\partial \alpha_5} & \frac{\partial P_Z}{\partial a_0} .. \frac{\partial P_Z}{\partial a_5} & \frac{\partial P_Z}{\partial d_1} .. \frac{\partial P_Z}{\partial d_6} \end{bmatrix}$, and

$\Delta E = [\Delta\theta_1 .. \Delta\theta_5 \;\; \Delta\alpha_0 .. \Delta\alpha_5 \;\; \Delta a_0 .. \Delta a_5 \;\; \Delta d_1 .. \Delta d_6]^T$. Equation (2.9) correlates the errors in the kinematics parameters with the pose errors. If both geometric and non-geometric factors causing the errors are considered while ignoring all other factors, then pose error can be described as:

$$\Delta P = J.\Delta E^{geom} + J.\Delta E^{non-geom} \tag{2.10}$$

Where, ΔE^{geom} and $\Delta E^{non-geom}$ are geometric (i.e. kinematics) and non-geometric parameters' error vectors respectively. Most of the previous research

directly corrected the kinematics parameters after the calibration. (Jang et al., 2001) suggested a variable error model to compensate for joints stiffness (i.e. one of the non-geometric parameter). However, none of the previous research has attempted to model and incorporated joints tilting errors in calibration, which could significantly affect a pose accuracy of serial robots. Therefore, this research would combine different kinematics models to develop a kinematics calibration model that would facilitate variable error compensation with sufficient parameters to incorporate joints tilting.

2.2 Measurement technologies

2.2.1 Fundamentals of measurements in robot calibration

Errors in some of the robot's parameters (such as joint twist, joint torques, and joint angles) can be measured directly by employing onboard sensors or can be approximated from the end-effector pose. The end-effector measurements can be positional (i.e. $P_a = [X\ Y\ Z\ ]^T$) or a full pose (i.e. $P_a = [X\ Y\ Z\ \Phi\ \theta\ \Psi]^T$) depending on the numbers of parameters considered during the calibration. The coordinates of one measurement target is enough to define the position of robot's end-effector. However, coordinates of three targets points on robot's end-effector are required to

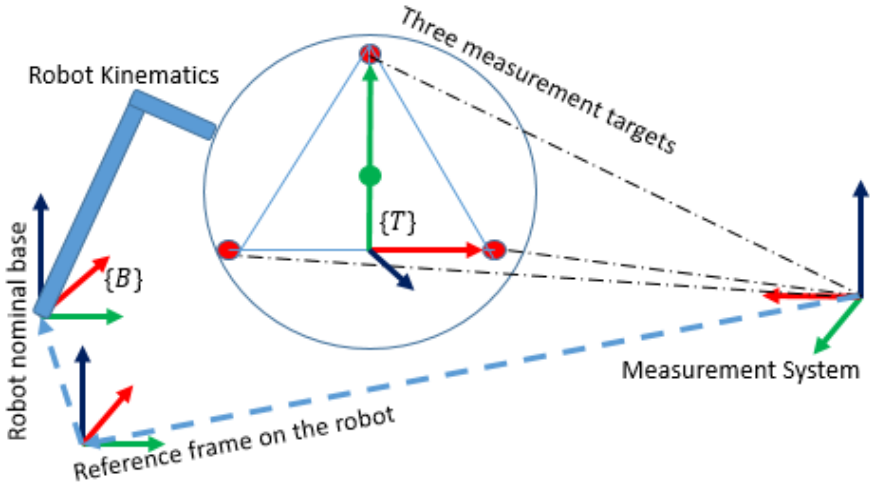

Fig. 2.2 Robot pose measurement

define absolute full pose of a robot end-effector. In other words, the formation of actual ${}^{Base}_{Tool}T$ in (2.3) requires coordinates of at least three points on robot's end-effector that can be arranged as shown in Fig. 2.2.

For the direct measurement of joint parameters, the serial robotics manipulators metrology uses the onboard sensors such as encoders and resolvers, shaft torque sensors, tactile sensors, temperature sensors, IMU's etc. Whereas, the end-effector's pose measurement can be further divided into absolute measurements and relative measurement. Laser distance sensors, vision systems and contact probes can be used for relative measurements of the dimensional quantities of the part that is being handled. Whereas, the measurements using laser and vision systems located away from the robots. This large volume metrology gives accurate information about the robot end-effectors absolute pose and hence used for the improvement of the absolute positioning accuracy of the robot. The following section reviews vision-based, close contact based, optical based and IMU based measurement technologies employed for the robot calibration.

2.2.2 Absolute measurement

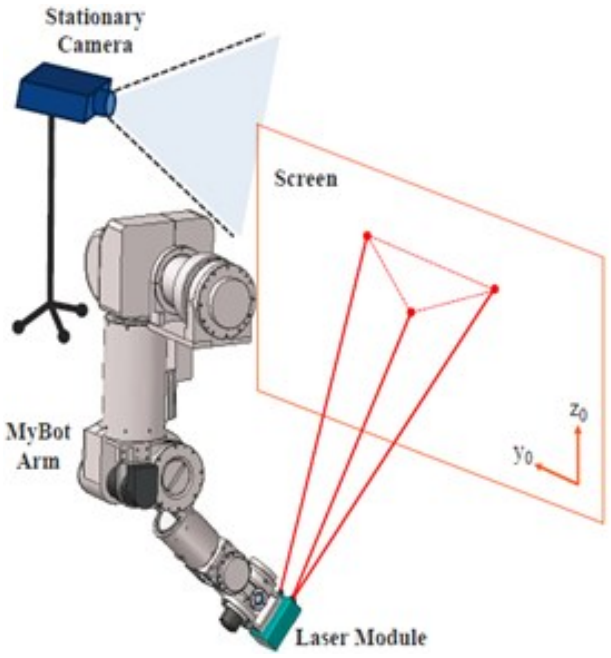

Fig. 2.3 Projection method
(Park and Kim, 2011)

The large volume metrology such as laser trackers, Optical CMM, and vision based systems are used for absolute pose measurement of robot end-effector. (Park and Kim, 2011) estimate full pose using vision system. The proposed technique uses CCD camera and a laser beam for robot calibration as shown in Fig. 2.3. Laser module attached on end-effector projects three laser beam on the screen. The stationary camera captures the position of the laser beams on the screen. Expected position of the beams

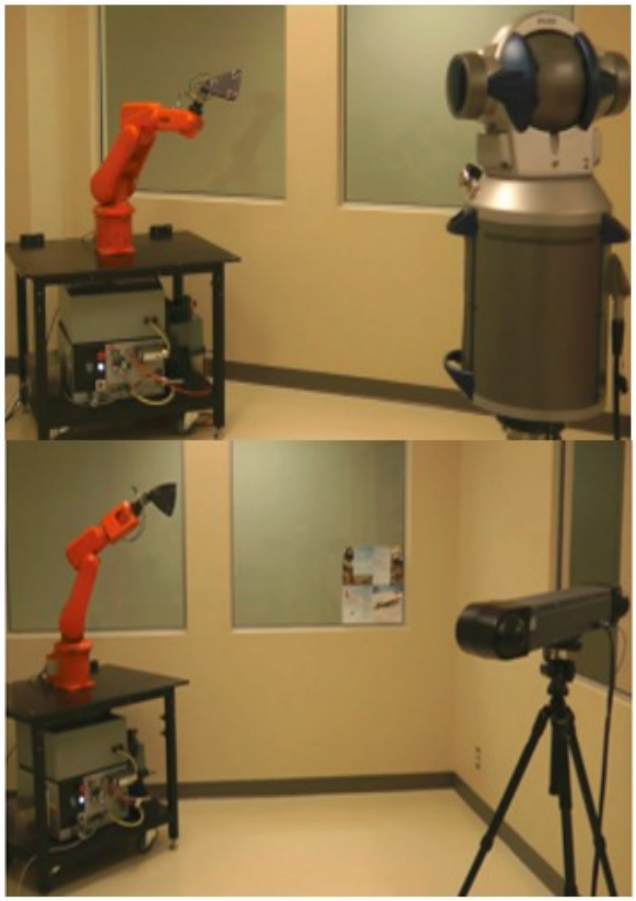

Fig. 2.4 Optical CMM and Laser tracker
Nubiola et al. (2014)

on the screen and captured positions are compared to correct the kinematics parameters. However, laser module itself needs to be calculated before attaching to the end-effector which indeed makes the calibration more time consuming and complicated. This technique also requires the sophisticated mathematical model to calculate the position of laser beams on screen and estimate the pose of robot end-effector. On the other hand, Meng and Zhuang (2007) attach the camera on robot end-effector, instead of rigidly fixing it in the workspace. Images of the chess-board are captured, and using a nonlinear factorisation method, end-effector poses are

calculated. By comparing measured poses and joint angle readings, the MCPC error model is prepared. The drawback of the proposed method is that distance between camera and chess-board must be known. Moreover, the chess-board must be relocated precisely for the measurements on different positions. Noise in the image, complex image processing, limited field of view and distance between the object and camera are the critical problems. Also limited by the camera resolution, and distortion calibration is necessary.

Nubiola et al. (2014) compare the most accurate and commercially available tools for calibration are laser trackers and optical CMMs shown in Fig. 2.4. He finds that the Laser trackers are accurate and have a broad range, but they are vulnerable to environmental conditions and extremely expensive (almost $120,000 US). Laser trackers can detect coordinates of one point at the moment, and must be used with spherically mounted reflectors which add additional cost. Moreover, laser tracker measures the position of its reference frame. Therefore, the precision of pose measurement concerning base frame decreases. On the other hand, optical CMMs (costs $ 90,000) can track the position and orientation (30 Hertz) and is easier to use. However, they are less accurate and measure up to a smaller volume. The presented work shows high accuracy in the calibration achieved for the ABB IRB120 robot. However, the extremely high cost and unease for an industrial environment keep these measurement methods limited to the laboratory environment.

2.2.3 Close loop formation

The relative measurements can be sufficient if the absolute position of the robot is not of interest. Švaco et al. (2014) attach two cameras perpendicular to each other to create a stereo vision and to form virtual TCP (Tool Centre Point). The proposed stereovision system captures two images of sphere independent of the viewing angle. Coordinates of a sphere centre are acquired in different configurations and from readings, absolute positioning errors are measured. The measurement data is used to correct the joint encoders offset values and thus should be called level 1 calibration. Whereas errors of the other joint link parameters are still ignored. Calibration results show improved accuracy, and error was decreased from 3.63 mm to 1.29 mm after the calibration procedure. However, the method is not convenient for calibration over the entire workspace as an object must be placed precisely at the number of known points. Due

to the limited field of view of a camera, poor accuracy and distortion in the image, the applications of camera based systems are limited in the calibration.

Nubiola et al. (2013) identifies the application of Renishaw Probes for the calibration, which was initially used for workpiece setup and measurements in CNC machines for calibration. With the help of contact plane and pre-defined movements, calibration has been performed on the PUMA 560 robot. All possible poses of end-effector are found using the forward kinematics of the hexapod arrangement as shown in Fig. 2.5. The moderate cost ($13,000.00) and the measurement accuracy (0.003 mm) found to be the most versatile. Although this method is most accurate, it requires too much human intervention and has a limited range up to 500mm only. The end-effector's movement is restricted by the movement of the ball-bar system and hence cannot be used to calibrate the robot over its entire workspace.

Fig. 2.5 Telescoping ball-bar
Nubiola et al. (2013)

Ge et al. (2014) presents low-cost and onsite calibration method using the ball, cubes and displacement sensor as shown in Fig. 2.6. Automatic calibration for tool coordinate and work coordinate is performed using the tip of displacement sensor which touch a fixed ball located in the workspace. The experiments are carried out on ABB IRB 140, and Levenberg-Marquardt method is used to approximate center of ball

and tool offset. The results indicated a significant improvement in relative position accuracy up to 0.03 mm, but further research is required for absolute kinematic parameters calibration. Repeat accuracy improves about 25%. However, kinematic parameters errors are not identified, which is the key to absolute accuracy. So, the improvement in the accuracy cannot be guaranteed over entire workspace of the robot.

Fig. 2.6 Contact probe on sphere
Ge et al. (2014)

Liu et al. (2009) recommend an alternatives method, where a laser pointer is mounted on the robot tool and Position Sensitive Device (PSD) is in the defined position shown in Fig. 2.7. The automated calibration includes targeting the laser lines at the center of the PSD surface (with focusing accuracy 0.25 um) from different robot's pose. The spotting is confirmed by accurate PSD feedback, which assures that each pair of laser lines meets at the same point. With the known PSD location with respect to the base frame and a single-point constraint, the close kinematic chain is formed. Joint angles are recorded and used to correct encoders offset (level 1 calibration). However, it is not possible to measure joint tilting errors with the proposed methodology. Indeed, joint offset errors result in tilting error for inclined postures of manipulators. Calibration improves the absolute positioning, but results remain limited as errors of kinematics parameters are not identified. The setup could be more effective if the laser

distance sensor is used instead of the laser beam. This would have provided accurate close formation for parameters identification. Wang et al. (2012) develops a similar procedure to measure position as well as the velocity of end-effector using Position Sensitive Detector (PSD) camera and an inertial sensor. Kinematic Kalman Filter (KKF) is used for fusion of data from PSD and IMU. Positional coordinates calculated by PSD are verified against CompuGauge (measurement system with 0.01mm

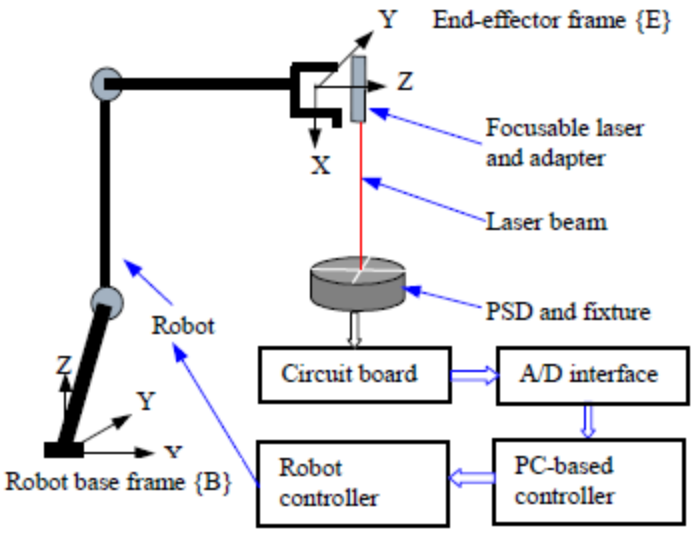

Fig. 2.7 Close loop formation with PSD
Liu et al. (2009)

accuracy). However, measurement noise and complexity of data fusion is the key issue in this measurement technique. It is evident that instead of relying on end-effector pose to estimate the joint parameters and errors, simultaneous detection of joint parameters can more effectively estimate the uncertainty in the robot calibration. Only position, velocity, and acceleration of the robot are estimated, and no detailed calibration results were provided in their research.

2.2.4 Direct measurements

Du and Zhang (2013) first proposes the online self-calibration method for robotic manipulator using IMUs. The IMU and peg were fixed on the robot end-effector to obtain the robot poses during motion as shown in Fig. 2.8. The camera captures an image when the robot is commanded to insert the peg into the hole on a steel plate. This allowed detection of angle and depth of insert. The measurements from the image are used further to modify the kinematics model. Cantelli et al. (2015) attaches IMUs

on each link along with the tool as shown in Fig. 2.9. The main purpose of the research is to find the pose of robotic manipulator without the use of joint encoders. Extended

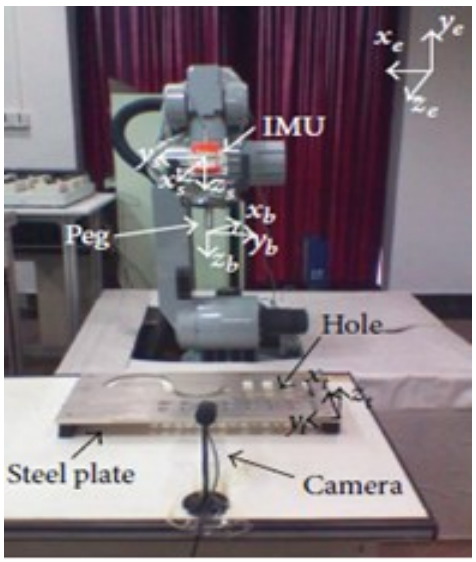

Fig. 2.8 IMU and camera
Du and Zhang (2013)

Kalman Filter was used to estimate pose from the IMUs data. It has been found difficult to estimate the angle of those joints whose axis of rotation is in or opposite direction of gravity. Moreover, considering the experimental results, this method cannot be used for high-precision application of manipulators calibration.

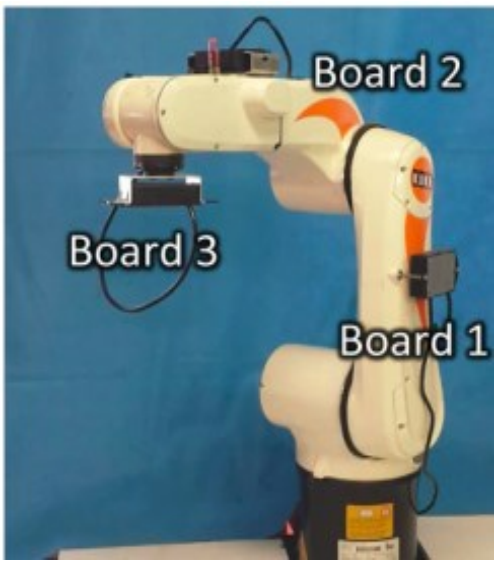

Fig. 2.9 IMU on each link
Cantelli et al. (2015)

All the IMU based techniques find orientation and position of robot end-effector and compare it against the orientation calculated using data received from the joint encoder

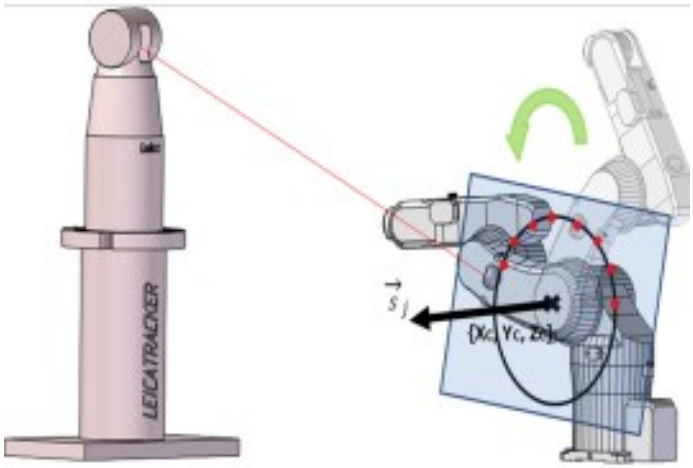

Fig. 2.10 Circle Point Analysis (CPA) using laser tracker
Santolaria and Ginés (2013)

to estimate kinematics parameters errors. Potential problems with IMU based calibration are the necessity of additional estimation algorithms, noise, and poor accuracy.

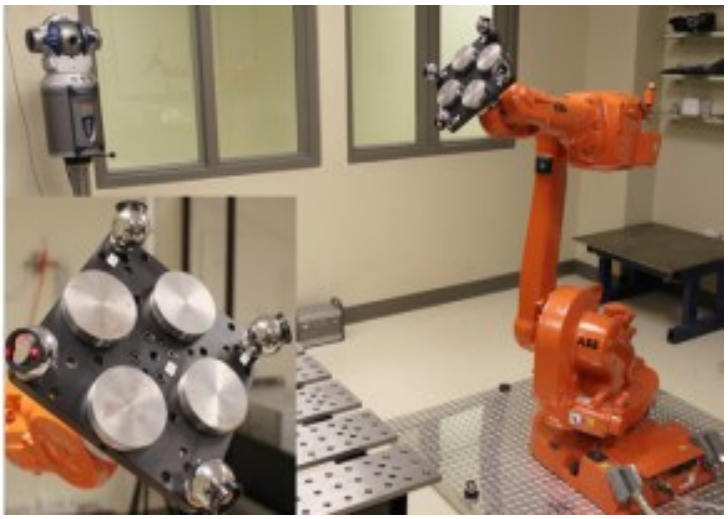

Fig. 2.11 CPA and full pose
(Nubiola and Bonev, 2013)

Santolaria and Ginés (2013) describes the CPA (Circle Point Analysis) to estimate the individual joint parameters while measuring the pose during the calibration process. Actual rotational axis is identified by approximating the plane perpendicular to the axis of rotation. This method shown in Fig. 2.10 requires complex hardware

setup and extremely expensive laser tracker, which is not suitable for onsite calibration. Further, CPA relies on interpolation to estimate the joint parameters. (Nubiola and Bonev, 2013) also use the CPA method to identify the axis of rotation for all the joints before building the nominal kinematic model for the calibration. Moreover, using Spherically Mounted Reflectors (SMRs) and laser tracker, they managed fully automate the measurement process as in Fig. 2.11. Least square estimation is used to identify 25 geometric error parameters and four joint compliance parameters for ABB IRB 1600 robot. The mean positional error reduced from 0.968 mm to 0.364 mm and the maximum positional error is reduced to 0.672 mm from 1.634 mm, which is best among all the calibration techniques. End-effector's pose can be measured accurately but still individual kinematics parameters errors are estimated.

2.2.5 Summary of the contemporary measurements methods

All the measurement methods used for the calibration of serial robotic manipulators are extremely expensive, require complex setup, frequent human. In the process of calibration, once the pose data is collected for various points within the workspace, the next step is to estimate the kinematics parameters errors which are responsible for the end-effectors pose errors. The selection of measurement equipment relies on the cost, accuracy, type of measurement (i.e. absolute, relative, positional, full pose etc.), and ease for the calibration. The process of identification of kinematics parameters errors is reviewed in the following section.

2.3 Errors identification

The third step of the robot calibration process is errors identification in various geometric and non-geometric parameters. (Wu et al., 2015) summarized various identification algorithms such as pseudo inverse, linear least squares, non-linear least squares, weighted pseudo inverse, Levenberg–Marquardt method, Genetic algorithm, and heuristic search method. Alternatively, some researchers propose direct compensation of the errors in cartesian space without identifying the errors in the robot’s parameters (Angelidis and Vosniakos, 2014). The errors identification methods are categorized as geometric errors identification, non-geometric errors identification, and non-parametric error identification (Chen-Gang et al., 2014).

2.3.1 Geometric errors identification

The geometric parameters errors (i.e. errors in joints angle, joints twist, links length and links offset) are largely responsible for the pose errors (Renders et al., 1991). (Heping et al., 2008) points out the significant effect of robot zero offsets (i.e. errors in the encoders readings while manipulator is at home position) on positional accuracy. He presents simplest and low-cost offset calibration method. The joint angles readings are recorded while manually tracking the laser line. The recorded joint angle values are then used to detect joint offset and correct encoders readings. However, the robot is operated manually during the tracking that causes alignment errors which ultimately results in the positioning errors. Moreover, only four kinematic parameters are used to describe the model which are insufficient to separate the effect of other error parameters on the joint offset. Level 1 calibration is performed to correct the encoders readings, and other kinematics parameters errors are neither identified nor considered. If the difference ΔP between the actual position $P_a = [X\ Y\ Z\ ]^T$ and the theoretic position $P_t = [X\ Y\ Z\ ]^T$ is known from the measurements, errors in the nominal kinematics parameters can be identified using the well-known pseudo inverse (Mooring et al., 1991) of (2.9) as:

$$\Delta E = \frac{J^T}{J \cdot J^T} \cdot \Delta P \tag{2.10}$$

Equation (2.10) is repeatedly used in the linearized least square a sense to find parameters error until the negligible positional error is achieved for each data point. The size $m \times n$ of mapping matrix J in (2.9) depends on the types of end-effector measurements and parameters to be identified. For example, if the only $[X\ Y\ Z\ ]$ coordinates of robot's end-effector are measured, then number of rows $m = 3$, and if it both position and orientation of the end-effector is measured, $m = 6$. Whereas, the number of columns n depends on the numbers of kinematics parameters error to be identified (i.e. numbers of elements in vector ΔE). Least square errors are calculated while considering the linearized model and ignoring the higher order non-linear errors terms, which compromise the estimation. The calibration result depends mostly on whether J has been accurately and sufficiently modeled (with geometric and non-geometric errors) and the accuracy of the sensor used. When $m < n$, the system becomes underdetermined, and we have infinite solutions and the best set of parameters are selected to improve overall accuracy. When $m > n$, the system

becomes overdetermined, and we cannot find an exact solution and the J becomes rank deficient. This happens due to the unidentifiable, poorly identifiable or linearly dependent parameters and singularities. This causes a problem when inverting J in equation (2.7). In such cases, numerical tools such as singular value decomposition (SVD) are used to eliminate parameter redundancies in the model (Meggiolaro and Dubowsky, 2000).

All the geometric errors identification methods ultimately find the set of kinematics parameters from end-effectors pose that can best fit the pose accuracy over the selected data points. The contemporary identification approaches do not find the actual errors in the nominal values of the kinematics parameters. Due to this, the improvement in the pose accuracy remains limited for few data points or region of the workspace. After calibration, errors of end-effector's position-related parameters are added directly, whereas errors of orientation related parameters are transformed into rotation error matrix and then compensated (Chen-Gang et al., 2014). After the calibration process has completed, the kinematic model with identified parameters can predict the actual tool pose more accurately. However, the modification to the nominal kinematics parameters is not allowed thus compensation is done through intermediate software and not in the firmware. It is found from the literature that constant error parameters are compensated after the calibration. However, the influence of some errors may depend on the pose, dynamics, and other factors and thus even though overall accuracy could be improved through contemporary compensation approaches, the errors might become worse at certain points and with certain robot configurations in the region.

2.3.2 Non-geometric errors identification

It is essential to consider nongeometric errors such as compliance errors besides geometric errors to attain the demanding accuracy for some of the robotic applications such as robotic laser cutting, robotic surgery, and robotic welding. Especially, joint clearance, joint compliance and backlash errors result into the configuration dependent joint tilting. The errors identification can be incorrect, if the joints tilting is not considered and compensated during the calibration. Gong et al. (2000) proposes a method to incorporate geometric errors, compliance and temperature variation in robot calibration. The joints have been modelled as a linear torsional spring to approximate the axial compliance. Temperature sensors were used to measure the thermal expansion of the links. However, the method does not explain how to separate

geometric joint errors and joint compliance form end-effectors pose measurement. Jang et al. (2001) divides the workspace into the small regions and uses Radial Basis Function Network (RBFN) to approximate the flexibility of joint as a function of workspace position. However, as the influence of joint errors is different at every single position, and hence its inverse approximation regarding workspace coordinates cannot be accurate.

Khalil and Besnard (2002) modifies the Newton Euler method to calculate the forces and moments acting at the links and joints to estimate the deformations of links and joints. However, their research ignores the pose errors due to joint clearance and

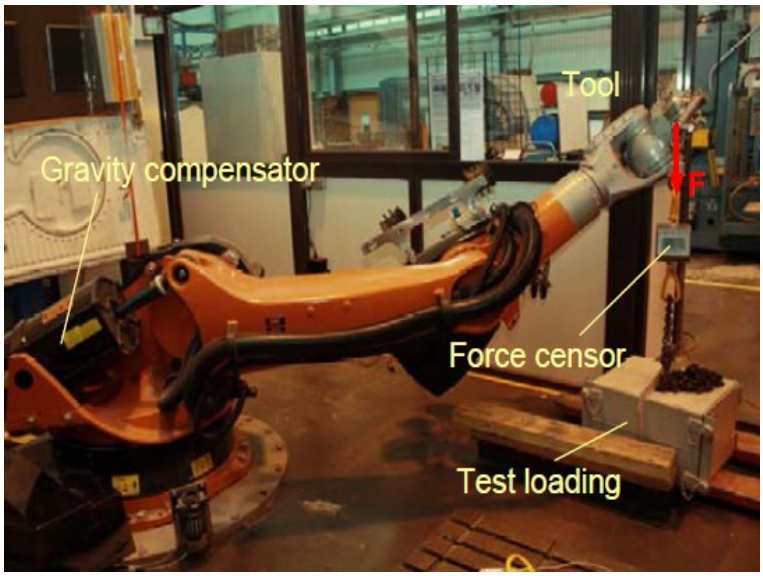

Fig. 2.12 Stiffness identification for the robot with gravity compensator (Klimchik et al., 2013)

backlash at the joints. Dumas et al. (2011) derives Cartesian stiffness matrix of the Kuka KR240-2 robot to compensate for the joints flexibility during the trajectory planning. However, their research ignores the geometric errors of the robot during the stiffness identification. Identification of joint stiffness can be crucial if the robot is heavy and equipped with the gravity compensators. Klimchik et al. (2013) experiments with a large industrial robot KR-270 as shown in Fig. 2.12. Joints deformation are predicted using identified joint compliance under the external loading.

He highlights that joint compliance for the joints close to the base can be precisely detected compare to the joints away from the robot base. The geometric errors are not identified and thus the prediction of end-effector pose by only considering the errors

due to stiffness on the mechanism can compromise the accuracy. Zhou et al. (2014) presented an algorithm for simultaneous identification of kinematics parameters errors

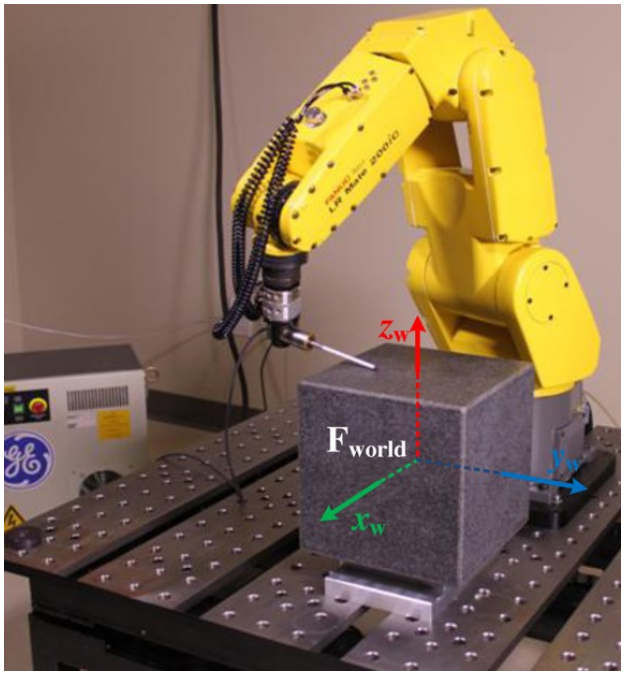

Fig. 2.13 Calibration by close loop formation
Joubair and Bonev (2015)

and positional errors due to axial compliance. However, their research ignores joint errors due backlash and joint clearance during the stiffness identification. Some of the non-geometric factors can be estimated using close loop formation by imposing the constraint on the robot end-effector. Joubair and Bonev (2015) form close loop multiplanar constraints using precision cube and contact probe for calibration as shown in Fig. 2.13. However, their research only identifies stiffness of the joints.

2.3.3 Non-parametric error identification

Artificial Intelligence (AI) techniques can be used in the calibration for optimum pose measurement, parameter identification and even to develop autonomous calibration procedure without human intervention. Xiao-Lin and Lewis (1995) suggested autonomous calibration based on robot's internal sensors. He uses Renishaw contact probe to detect orthogonally located contact plane, and forms close loop for position measurement. Recurrent Neural Network (RNN) is used to identify the joint parameters which is computationally more efficient than the standard linear least square methods. It is evident that error parameters vary over the entire workspace of

the manipulator. Moreover, Calibrated Error Parameters (CEPs) are accurate only in certain region of the workspace. Another application of NN (Neural Network) for robot calibration has been identified by (Jang et al., 2001). Like earlier, the workspace is divided into small regions and pose measurements have been carried out for the selected regions of manipulator's workspace respectively. Radial Basis Function Network (RBFN) has been developed to estimate calibration errors in remaining regions. However, errors of only first three joints have been investigated. Moreover, the trajectory selected for the validation of their method passes through the centers of cubes, otherwise, may result in the poor error estimation.

Ha (2008) estimates joint error parameters using relative position errors. He examines the difference between actual positions of end-effector for two different command pulses. The experiments have been performed on MOTOMAN UP20 robot. However, the accuracy of the measurement system in X and Y direction is restricted to 0.1 mm due to grid resolution and 0.01 in the Z direction (height sensor). Even though the five joint error parameters have been identified, this method relies on Least Square Estimation to find optimum kinematic parameters which do not present actual joint parameters. Zhao et al. (2015) also proposed Calibration Based Iterative Learning Control (CILC) based method for path tracking. Parameters are corrected from previous tracking results. The purpose of the study is to improve iterative learning control which used in path tracking of industrial robots. This is achieved through kinematics parameters modification from previous tracking results. Experiments have been carried out on ABB IRB 4400 and position data has been captured using BIG 3D FP700. However, this method requires expensive laser trackers and complex measurement set up. Improvement remains limited up to tracked trajectory. Recently, Wu et al. (2015) come up with an idea of enhanced partial pose measurement. They introduced an additional step of the design of experiment in the convention calibration process to ensure maximum positional accuracy. A considerable improvement in positional accuracy of KUKA KR-270 robot has been observed with the help of test-pose based approach. This method relies on many positional data points to avoid non-homogeneity of identification equations. There is no clear procedure to identify robot zero reference frame is indicated. Furthermore, proposed technique demands a large set of position coordinates which makes the measurement process lengthier. All the AI techniques discussed above deals with parameter identification stage of the calibration process. The key role of this techniques is still to the optimum fitting of data. The

application of AI techniques may be more effective to predict errors due to other factors such as noise, temperature, and control errors instead of an approximation of geometric parameters. The AI techniques can be more efficiently used in automating the calibration procedure rather than identification of errors.

2.4 Errors compensation

Compensation of the errors in the nominal kinematics model is the last phase of a robot calibration. Errors compensation relies on the kinematics error model selected for the calibration. For example, if the original theoretical kinematics model has 4 parameters in link transformation then maximum of 4 errors can be compensated. Conventional geometric calibration directly modifies a theoretical kinematics model of the robot once errors in kinematics parameters are detected. On the other hand, non-geometric calibration employs variable error compensation (i.e. to compensate for joints stiffness).

2.5 Summary

Kinematics parameters' error identification based on a set of end-effectors data cannot find the exact values of kinematics parameters. The kinematics parameters error is identified (i.e. indeed approximated) from a set of end-effector data are not consistent with all the data points of the workspace. Constant error compensation limits the improvement up to a few point or region of the workspace. None of the research has considered the level of impacts on pose errors caused by different parameters during the errors identification at a given pose. Joints tilting due to clearance, backlash, and flexibility is not addressed in previous researches. None of the research has proposed mathematics required to model joints tilting behavior. Even efficient kinematics models such as MCPC and POE model have never been used to incorporate joints tilting during the calibration. Due to the serial connection of links, joints tilting errors indeed have the highest and posture dependent influence on the pose accuracy. Complex measurement setup limits the calibration process within the laboratory environment. Moreover, accurate measurement equipment like laser tracker sometimes cost more than the cost of the robot itself. Intense human intervention and skills are required. Most of the calibration processes are time-consuming.

2.6 Gap

(1) Standard geometric errors identification does not account for the configuration dependent influence of kinematics parameters errors on pose accuracy during a robot calibration.

(2) Contemporary robot calibration does not consider joints tilting and thus cannot improve pose accuracy above certain level.

2.7 Aims and Objectives

This research is aimed at improving the effectiveness of a robot calibration by considering the level of influences on pose errors caused by different parameters and joints tilting during the calibration. Therefore, the objectives of this research are as follows.

(1) To analyze the configuration dependent influence of kinematics parameters errors on positional accuracy, and to propose and validate influence based geometric error identification.

(2) To propose a mathematics required to incorporate joints tilting in the calibration of serial robotic manipulators. The proposed approach would be applied to improve absolute pose accuracy as well as trajectory tracking accuracy of a robot with the help of a low-cost measurement set-up.

CHAPTER 3 INFLUENCE BASED ERRORS IDENTIFICATION

In serial robotic manipulators, due to the nature of the coupling of links, the influence of errors in joint parameters on pose accuracy varies with the configuration. Kinematics parameter's error identification in the standard kinematics calibration has been configuration independent which does not consider the influence of kinematics parameters' error on robot accuracy (Chen-Gang et al., 2014). Mutually dependent joint parameter errors cannot be identified at the same time, and hence error of one parameter in each pair is identified (Zhou et al., 2014). In a pair of mutually dependent joint parameters, the effect of error in one parameter on positional error can be more than the other one depending on the configuration. Therefore, the error detection may be incorrect if the influence of joint parameters is ignored during the error identification. This chapter analyses the configuration dependent influences of kinematics parameters error on pose accuracy of a robot. Based on the effect of kinematics parameters, the errors in the kinematics parameters are identified. Kinematics model of the robot is composed of the modified DH method and an improved DH method to avoid the limitations of the original DH method. First, the robot is calibrated to identify errors in 17 kinematics parameters conventionally, and then errors are detected based on the proposed method.

3.1 Difficulty with the conventional errors identification

An error identification in the contemporary kinematics calibration simultaneously approximate the errors of all kinematics parameters using methods such as linear least squares, non-linear least squares, pseudo-inverse, genetic algorithm, and heuristic search method (Wu et al., 2015). This process is repeated for few selected configurations to calculate a set of kinematics parameters which best fit the accuracy to all selected configurations. However, different pose errors occur for the same individual joint parameter over various configurations. For example, in Fig. 3.1, θ_1, θ_2, and θ_3 are mutually dependent parameters whose errors cause positional error at end-point P. In configuration 1 (i.e. P_1), θ_1 is more influential than θ_2, and opposite in configuration 2 (i.e. P_2). Therefore, during the error identification more influential parameter in each pair must be considered at every selected configuration. However,

contemporary error identification ignores the configuration dependency of the influence of kinematics parameters on a pose accuracy which leads to incorrect error identification at certain configurations of a robot. The following section prepares kinematics model of the Katana 450 robot.

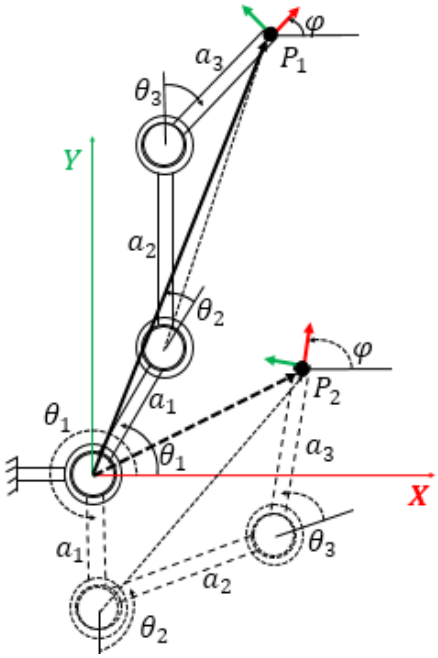

Fig. 3.1 Mutually dependent parameters with variable influence

3.2 Kinematics modelling of the Katana 450 robot

This research combines the modified DH method and improved DH method to retain continuity of kinematics model of the robot considering the nominal values of the kinematics parameters listed in Table 1. In the modified DH method, the frame i is rigidly attached to the link i, which rotates around joint i. The transformations ${}^{i-1}_{i}T$ between the frames $(i-1)$ and i is described with the help of two rotational parameters α_{i-1} and θ_i, and two translational parameters a_{i-1} and d_i.

Table 3.1 Kinematics parameters of Katana 450

Joint i	$\alpha_{i-1}{}^{o}$	a_{i-1} *mm*	$\theta_i{}^{o}$	$\beta_{i-1}{}^{o}$	d_i *mm*
1	0	0	+/-169.5	-	0
2	90	0	+102 / -30	-	0
3	0	190	+/-122.5	0	-
4	0	139	+/-112	0	-
5	-90	0	+/-168	-	147.3
6	90	0	Inactive	-	200

Therefore, the homogeneous link transformation matrix ${}^{i-1}_{i}T$ is obtained using the following transformations as:

$$ {}^{i-1}_{i}T = Rot(X,\alpha_{i-1})Trans(X,a_{i-1})Rot(Z,\theta_i)Trans(Z,d_i). \tag{3.1} $$

$$ = \begin{bmatrix} c(\theta_i) & -s(\theta_i) & 0 & a_{i-1} \\ c(\alpha_{i-1})s(\theta_i) & c(\alpha_{i-1})c(\theta_i) & -s(\alpha_{i-1}) & -d_i\, s(\alpha_{i-1}) \\ s(\alpha_{i-1})s(\theta_i) & s(\alpha_{i-1})c(\theta_i) & c(\alpha_{i-1}) & d_i\, c(\alpha_{i-1}) \\ 0 & 0 & 0 & 1 \end{bmatrix} $$

Joint 2,3 and 4 are parallel so the improved DH method must be employed with an additional parameter β to correlate frames 2,3 and 4 to avoid discontinuity. The transformation matrix is obtained using transformations:

$$ {}^{i-1}_{i}\boldsymbol{T} = Rot(X,\alpha_{i-1})Rot(Y,\beta_{i-1})Trans(X,a_{i-1})Rot(Z,\theta_i). \tag{3.2} $$

Eq. (3.2) correlate frames 2,3 and 4 using $\boldsymbol{T^2_3}$ and $\boldsymbol{T^3_4}$. The improved H method avoids the limitations of the modified DH method. The transformation ${}^{0}_{6}T$ between the robot

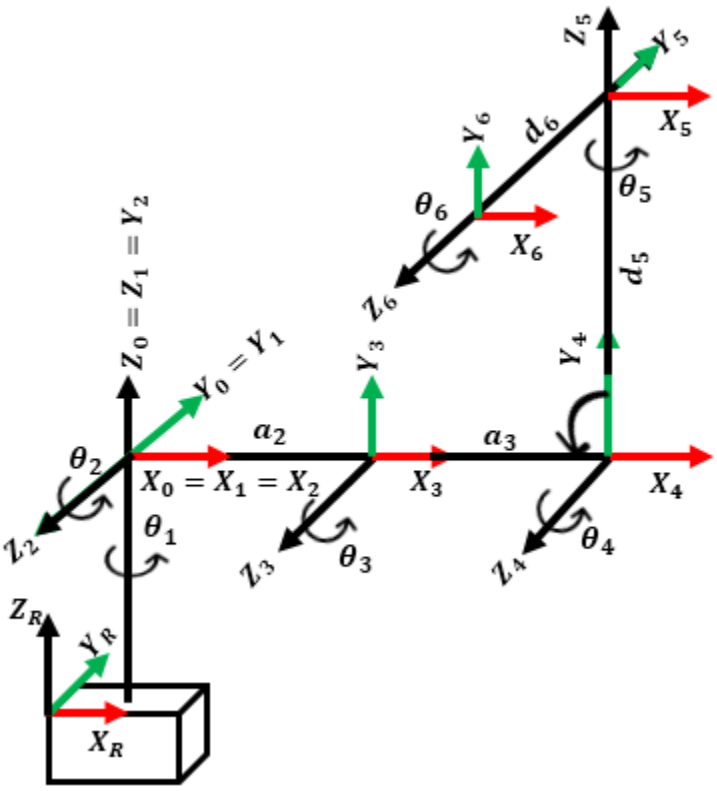

Fig. 3.2 Frames Assignment for Katana 450

base and the robot end-effectors is obtained by putting values of joint link parameters of Table 1 into transformation matrices as:

$$ {}^{0}_{6}T = {}^{0}_{1}T \cdot {}^{1}_{2}T \cdot \mathbf{{}^{2}_{3}T} \cdot \mathbf{{}^{3}_{4}T} \cdot {}^{4}_{5}T \cdot {}^{5}_{6}T \tag{3.3} $$

The homogeneous transformation matrix ${}^{0}_{6}T$ in (3.3) describes pose (i.e. position and orientation) of the robot end-effectors on the robot's nominal base. The kinematics model of the Katana 450 robot describes orientation of robot's end-effector as ZXZ Euler angles Φ, θ, and Ψ . Therefore, the pose P of robot is defined by the coordinates X, Y, and Z and orientation angles Φ, θ, and Ψ in the form of vector $P = [X \ Y \ Z \ \Phi \ \theta \ \Psi]^T$. The derived kinematic model of the robot has been verified against the robot's control software. For the calibration purpose, the positional error vector ΔP between the actual pose P_a and the theoretical pose P_t of the end-effectors can be described as:

$$ \Delta P = P_a - P_t = [\Delta X \ \ \Delta Y \ \ \Delta Z \ ]^T \tag{3.4} $$

The following section compares various large volume metrologies for selecting an appropriate technology to measure actual pose of the robot in (3.4).

3.3 Comparison of measurement technologies and experimental setup

Firstly, the laser tracker has been used which can measure coordinates of the single point at a time or track the single target continuously as shown in Fig. 3.3. The

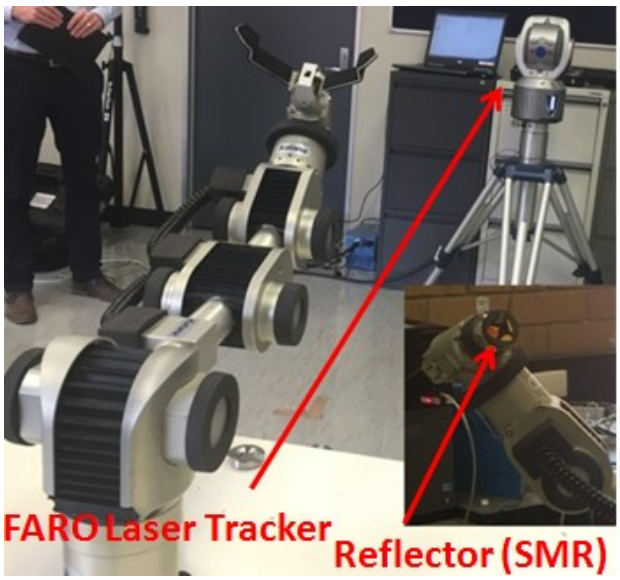

Fig. 3.3 Faro Laser Tracker

additional artifacts with multiple SMR will be required to obtain full pose of end-effector. The volumetric accuracy of laser tracker is 20 microns within 10 meters, which is the most accurate in all available technologies. The thickness of SMR adaptor shown in Fig. 3.3 is auto compensated in the software. However, the laser beam was obstructed when robot tool pose is beyond 45° of the line of sight, and could not measure the coordinates of SMR. The measurements of laser tracker indicated the positional accuracy of Katana can be as poor as 2.11 mm which is far poor at some poses.

Secondly, Creaform C-Track has been used to measure the same 30 data points. The system comes with a handy probe that can be tracked as well as used to define reference coordinates for the measurement as shown in Fig. 3.4. C-Track can track multiple passive targets (reflector) and hence can be used for continuous full pose measurement. The accuracy of C-Track is 60 microns. Measurements of C-track are susceptible to temperature change, and attachment of three measurement targets to form coordinate system for full pose measurement was found to be difficult.

Fig. 3.4 C-Track measurement system

Finally, the NDI Optotrack was used for the pose measurement at same 30 points in robot workspace. Optotrack is capable of continuously tracking multiple active targets. The optical marker was used to define the reference coordinates for the measurements shown in Fig. 3.5. Three signature LED were attached on robot's end-effector whereas another three were attached to the table as shown in Fig. 3.5. Optotrack gives coordinates of stationary marker points and three signature LEDs as well as three target signature LEDs, and thus capable of continuous full pose

measurement. The volumetric resolution of Optotrack is 0.01 mm within 2 to 7 meters and cannot measure in 0 to 2 meters. The coordinates of stationary signature LEDs attached on the table was not needed in pose measurement and just used to define markers' coordinates. The pose information acquired by Optotrack is coordinates of three signature LEDs. Thus, the average value of X, Y, and Z coordinates of all three LEDs was considered to find coordinates of the center of three LEDs, which is indeed the TCP of our measurements. With digitizing probe (i.e. optical marker in Fig. 3.5),

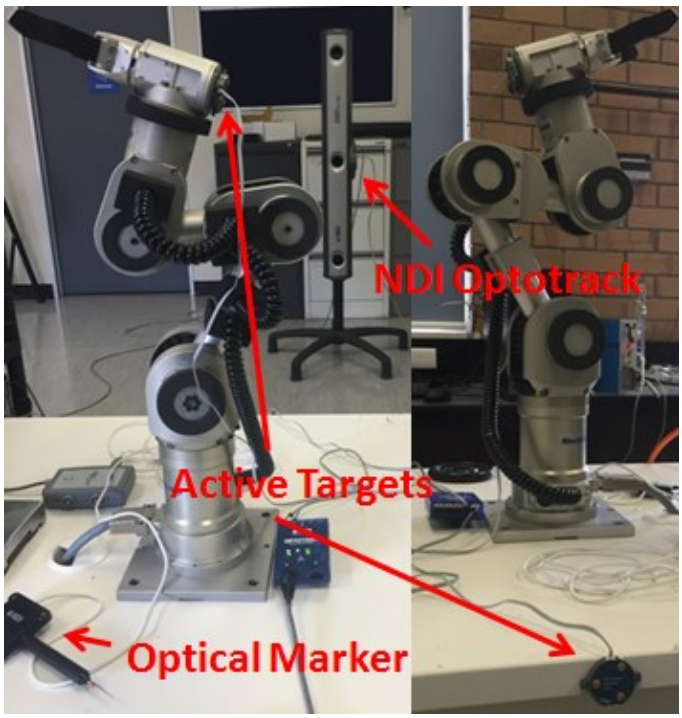

Fig. 3.5 NDI Optotrack with active targets

it is relatively easy to mark reference coordinate system anywhere on the robot. Moreover, three active targets on the fixed structure easily provides a full pose of a robot. Considering the advantages, NDI Optotrack system has been used for the validation of improvement in the accuracy of the Katana 450 robot in this research.

The experimental setup includes a five DOF Katana 450 robot, an Optotrack system with a volumetric resolution of 0.01 mm, active vibration isolation table, and a computer to control the robot. The end link of the Katana 450 robot is 118 mm long gripper, which is replaced with the 200 mm long and 0.5 Kg tailored attachment shown in Fig. 3.6. The attachment imitates maximum payload of the robot, provide the ease for attaching the measurement targets, and amplify the joint errors due to a larger length. The digitizing probe shown in the top-left corner of Fig. 3.6 used by the

Optotrack system, it is easy to establish the global coordinate system for the measurements. The system measures Cartesian coordinates of three active markers on the established global coordinates system at the structural base of the robot. The coordinates of three markers are used to calculate the position as well as the orientation of the robot's end-effector on the structural base of the robot as shown in Fig. 3.6. The translational transformation of [55 55 201.5]' mm transforms the coordinates of the structural base to the robot's nominal base as per design specification of the robot.

Fig. 3.6 Experimental set-up

3.4 Katana Native Interface (KNI) and GUI

For this research, the robot is controlled with the MATLAB using Katana Native Interface language for the calibration, measurements, and modification of the kinematic parameters after the calibration. The Graphical User Interface (GUI) developed in this research, shown in Fig. 3.7 facilitates basic movement from one pose to another by defining either pose or joint angles using forward and inverse kinematics in the back end. The poses can be defined and recorded before and after the calibration.

Also, circular or linear trajectories can be defined, and the robot can be commanded to follow the same. The next step is to select the poses for the measurements. Due to the nature of the forward kinematics model of serial robots, the pose errors are similar when the robot configurations are close (Tian et al., 2015). Therefore, the coordinates of 118 poses are selected within the largest cube of the robot's workspace as per proposed performance criteria and related test methods in the ISO 9283:1998 (Johnsrud, 2014) for the robotic manipulators. The measurements are sequenced such that all five joints angle change when moving from one pose to another. The following section analyses influence of kinematics parameters at each selected pose.

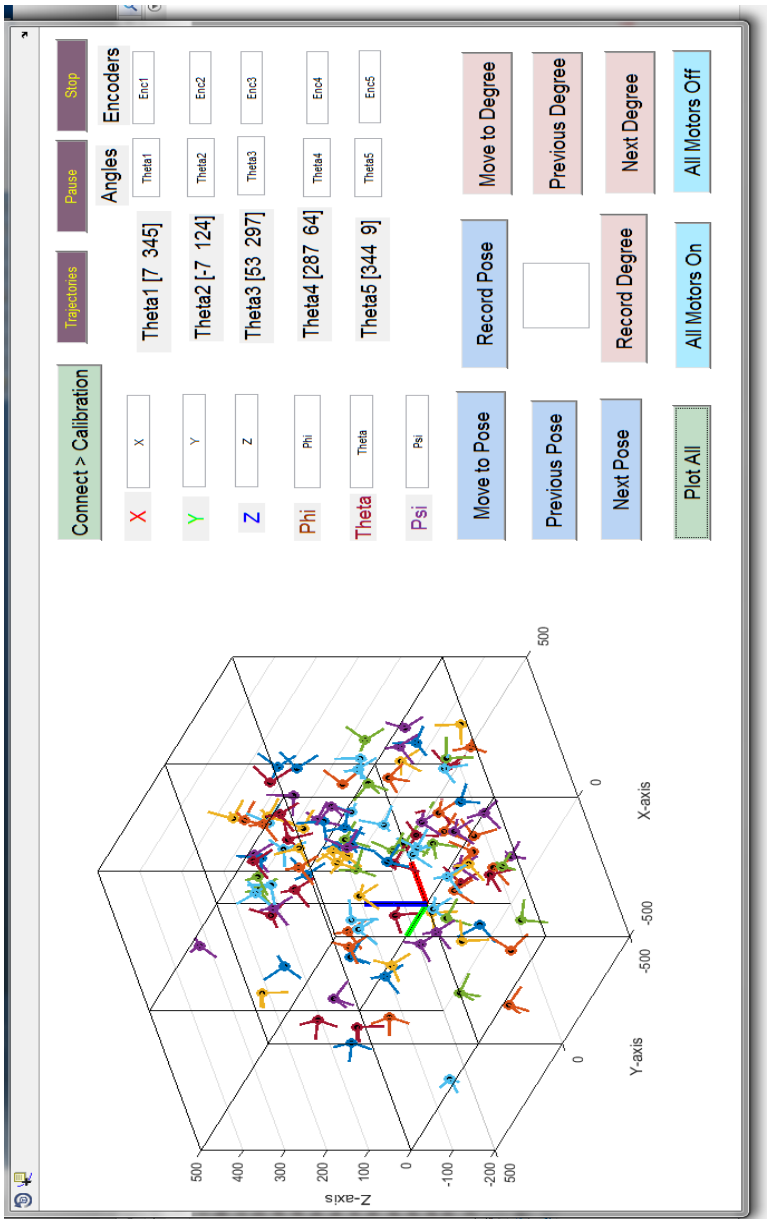

Fig. 3.7 Katana Native Interface and GUI

3.5 Analysis of influence of kinematics parameters

A deviation of +0.05 on angular parameters ($\theta_i \ldots, \alpha_i \ldots \beta_i \ldots$) and +0.1 mm on linear parameters ($a_i .., d_i ..$) is imposed at data points (i.e. configurations) shown at the bottom half of Fig. 3.7. Simulation of the effect of deviations in kinematics parameters on robot end-effector provided the influence of each kinematics parameter for a given robot configuration. Same process is repeated over 118 configurations. The error of +0.1 mm in linear parameters causes an absolute positional error of 0.1 mm regardless of the configuration of the robot. However, an error of +0.05° in rotational parameters causes configuration dependent error on end-effectors position as shown in Fig. 3.8. The common understanding is the influence of rotational parameters error decreases from the base towards end-effector in serial robot, i.e. error in θ_2 has a larger impact on positional accuracy than θ_3. However, error in θ_3 (for example, θ_3 maximum in Fig. 3.8) can have a larger impact on positional accuracy than θ_2 (for example, θ_2 minimum in Fig. 3.8) for some configurations as per analysis in Fig. 3.8. Therefore, followings section proposes influence based error identification of kinematics parameters error.

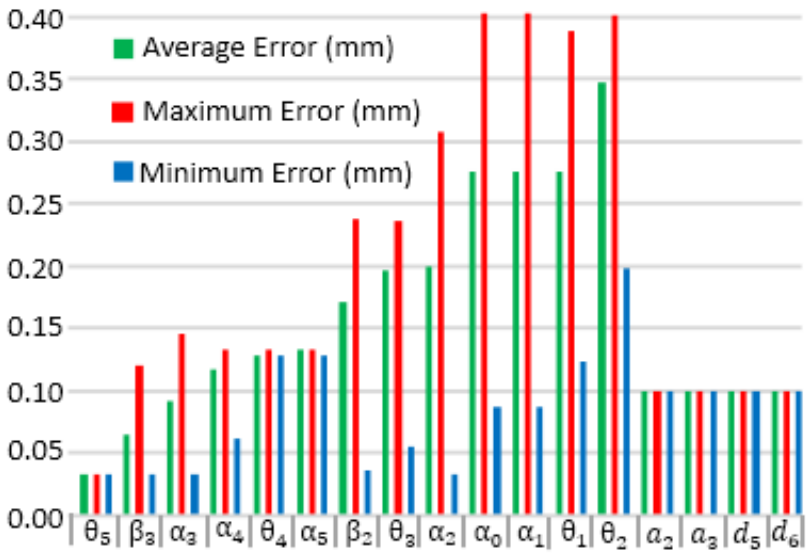

Fig. 3.8 Influence of kinematics parameters

3.6 Standard Vs Proposed Influence based errors identification

For the calibration purpose, positional errors vector $\Delta P = [\Delta X \ \Delta Y \ \Delta Z]$ is correlated to the kinematics parameters error vector ΔE with the help of the mapping matrix J as:

$$\Delta P = J.\Delta E. \tag{3.5}$$

Where, $J = \begin{bmatrix} \frac{\partial P_X}{\partial \theta_1} .. \frac{\partial P_X}{\partial \theta_5} & \frac{\partial P_X}{\partial \alpha_0} .. \frac{\partial P_X}{\partial \alpha_5} & \frac{\partial P_X}{\partial \beta_2} \frac{\partial P_X}{\partial \beta_3} & \frac{\partial P_X}{\partial a_3} \frac{\partial P_X}{\partial a_4} & \frac{\partial P_X}{\partial d_5} \frac{\partial P_X}{\partial d_6} \\ \frac{\partial P_Y}{\partial \theta_1} .. \frac{\partial P_Y}{\partial \theta_5} & \frac{\partial P_Y}{\partial \alpha_0} .. \frac{\partial P_Y}{\partial \alpha_5} & \frac{\partial P_y}{\partial \beta_2} \frac{\partial P_y}{\partial \beta_3} & \frac{\partial P_Y}{\partial a_3} \frac{\partial P_Y}{\partial a_4} & \frac{\partial P_Y}{\partial d_5} \frac{\partial P_Y}{\partial d_6} \\ \frac{\partial P_Z}{\partial \theta_1} .. \frac{\partial P_Z}{\partial \theta_5} & \frac{\partial P_Z}{\partial \alpha_0} .. \frac{\partial P_Z}{\partial \alpha_5} & \frac{\partial P_X}{\partial \beta_2} \frac{\partial P_y}{\partial \beta_3} & \frac{\partial P_Z}{\partial a_3} \frac{\partial P_Z}{\partial a_4} & \frac{\partial P_Z}{\partial d_5} \frac{\partial P_Z}{\partial d_6} \end{bmatrix}$ and

$$\Delta E = [\Delta\theta_1 .. \Delta\theta_5 \ \ \Delta\alpha_0 .. \Delta\alpha_5 \ \Delta\beta_2 \ \Delta\beta_3 \ \ \Delta a_3 \ \Delta a_4 \ \ \Delta d_5 \ \Delta d_6 \ ]^T.$$

Eq. (3.5) correlates the kinematics parameters error vector ΔE with the positional error vector ΔP. Firstly, the kinematics parameters' errors are identified using the unique least square estimation (Roth et al., 1987) as:

$$\Delta E = \frac{J^T}{J \cdot J^T} \cdot \Delta P \tag{3.6}$$

Eq. (3.6) is iteratively used at each pose to correct the kinematics parameters error. In each iteration, a new ΔE is obtained which is compensated in (3.5) to obtain new ΔP. Iterations are repeated till the positional error is detectable by the measurement equipment being used (i.e. above 0.01 mm in this case) for the calibration. The same procedure identifies the kinematics parameters' errors for all poses. From the sets of errors in the kinematics parameters of all poses, a set of kinematics parameters is calculated that best fit the accuracy to all measured poses. However, the error detection may be incorrect if influence is not considered during the error identification. For example, in the configuration $\theta_1, \theta_2, \theta_3, \theta_5 = 0$ and $\theta_4 = 80^0$ influence of θ_4 is larger than θ_3.The positional error ΔP can be corrected by correcting θ_3 or θ_4. Even if influence of θ_4 is larger than θ_3 for that configuration, the conventional identification may identify larger error of θ_3 instead of smaller error in θ_4 for the same positional error ΔP. This incorrect identification of large error in θ_3 at this configuration would affect the set of best fit parameters in the end. Additionally, incorrect identification at few configurations may lead to significant positional error at uncalibrated points.

Therefore, this research employs coefficient C<1 in (3.8) to increase the numbers of iterations for errors identification at each pose. At each pose, in each of the iteration, error vector ΔE is multiplied influence vector $k = [k_1 .. k_{17}]$ as:

$$\Delta P = J.(\Delta E k), \tag{3.7}$$

and subsequent error vector ΔE is calculated as:

$$\Delta E = C\ \frac{J^T}{(JJ^T)} \cdot \Delta P. \tag{3.8}$$

Where, $k = [k_1..k_{17}]$ is obtained from the influence of kinematics parameters at a pose as explained in the Section 3.5. For example, consider that the parameters influence at one of the configuration is like average influence of kinematics parameters shown in Fig. 3.8. In this case θ_2 is the most influential with nearly 0.34 mm error leads to $k_2 = 1$. For this configuration, 0.34 mm is considered as 100%, and values for the remaining ks in that configuration can be found with reference to k_2. Like $k_8 = 0.59$ for α_2. For some of the configurations, where only θ_1 changes, vector k remains same, otherwise changes with the configurations. The proposed approach for error identification increases the computational cost, however, with the availability of low cost and faster computing power, an accurate error identification is desired. The following section discusses the calibration results obtained using both conventional and influence based error identification approach.

3.7 Experimental results and conclusion

Table 3.2 and Table 3.3 lists errors of 17 kinematics parameters identified with standard method and influence based approach respectively, and Table 3.4 compares the improvement in pose accuracy in term of various pose parameters. The overall positional accuracy improves significantly using proposed method for error identification. The current identification could reduce average positional error from 1.21 mm to 0.38 mm whereas influence based identification reduced error from 1.21 mm to 0.21 mm. Even though the orientation errors are not identified, the measurements show improvement in orientation accuracy as well.

The proposed approach for the identification of kinematics parameters errors has proven to be effective compared to the standard one. Consideration of influence of kinematics parameters during an error identification improved positional accuracy of a robot by nearly 14%. This approach can be further developed for improving the dynamic pose accuracy of the serial robotic manipulators.

Table 3.2 Standard simultaneous identification

Joint i	$\alpha_{i-1}{}^{o}$	a_{i-1} *mm*	$\Delta\theta_i{}^{o}$	$\beta_{i-1}{}^{o}$	d_i *mm*
1	0	-	-0.061	-	-
2	89.92	-	0.0232	-	-
3	0.003	190.003	-0.057	0.0021	-
4	0.007	139.01	0.0641	0.0013	-
5	-90.01	-	-0.121	-	147.302
6	90.03	-	-	-	200.001

Table 3.3 Proposed influence based identification

Joint	$\alpha_{i-1}{}^{o}$	a_{i-1}	$\Delta\theta_i{}^{o}$	$\beta_{i-1}{}^{o}$	d_i *mm*
1	0	-	-	-	-
2	90.0	-	0.03	-	-
3	-	190.0	0.06	0.005	-
4	0.06	139.0	0.02	-	-
5	-	-	-0.01	-	147.30
6	90.0	-	-	-	200.00

Table 3.4 Calibration results

Average over 118 positions			
Pose parameter	Before the calibration	Simultaneous identification	Influence based identification
$\lvert\Delta X\rvert$	0.63	0.28	0.18
$\lvert\Delta Y\rvert$	0.44	0.13	0.10
$\lvert\Delta Z\rvert$	0.85	0.25	0.16
$\lvert\Delta P\rvert$	1.21	0.38	0.21
$\lvert\Delta\Phi\rvert°$	0.27	0.096	0.088
$\lvert\Delta\theta\rvert°$	0.17	0.027	0.022
$\lvert\Delta\Psi\rvert°$	0.26	0.084	0.079

CHAPTER 4 JOURNAL PAPER 1

Statement of Authorship

Title of Paper	**Investigation of Influence of Joints Tilting for Calibration of Serial Robotic Manipulators**
Publication Status	☐ Published ☐ Accepted for Publication ☑ Submitted for Publication ☐ Unpublished and Unsubmitted work written in manuscript style
Publication Details	PATEL, D., LU, T.-F. & CHEN, L. 2017. Investigation of Influence of Joints Tilting for Calibration of Serial Robotic Manipulators. *International Journal of Precision Engineering and Manufacturing.*

Principal Author

Name of Principal Author (Candidate)	Dhavalkumar Patel		
Contribution to the Paper	Established concept, derived mathematics, performed experiments, interpreted data, wrote manuscript and acted as corresponding author.		
Overall percentage (%)	60 %		
Certification:	This paper reports on original research I conducted during the period of my Higher Degree by Research candidature and is not subject to any obligations or contractual agreements with a third party that would constrain its inclusion in this thesis. I am the primary author of this paper.		
Signature		Date	21 NOV 2017

Co-Author Contributions

By signing the Statement of Authorship, each author certifies that:

i. the candidate's stated contribution to the publication is accurate (as detailed above);

ii. permission is granted for the candidate in include the publication in the thesis; and

iii. the sum of all co-author contributions is equal to 100% less the candidate's stated contribution.

Name of Co-Author	Tien-Fu Lu		
Contribution to the Paper	Supervised development of work, helped in data interpretation and manuscript evaluation.		
Signature		Date	23/11/2017

Name of Co-Author	Lei Chen		
Contribution to the Paper	Helped to evaluate and edit the manuscript.		
Signature		Date	28/11/17

Title: Investigation of Influence of Joints Tilting for Calibration of Serial Robotic Manipulators

Dhavalkumar Patel, Tien-Fu Lu and Lei Chen

School of Mechanical Engineering, University of Adelaide, Adelaide 5005, Australia

Keywords: Calibration, Error identification, Joint tilting, Measurement, Pose accuracy, Serial robots

Abstract

Pose accuracy of serial robotic manipulators could be heavily influenced by joint tilting that occurs due to joint clearance, backlash and joint flexibility. Errors identification in conventional calibration relies on the robot end-effector pose, which may not improve the pose accuracy of a robot above a certain level if the tilting of joints is ignored during error identification. To reveal the influence of joints tilting which has not been carefully considered in literature, this research models configuration dependent joint tilting and presents a novel method to encapsulate them in the calibration of serial robotic manipulators. The kinematics model of robot is modified such that geometric joint errors, as well as joint tilting, can be identified and compensated using the kinematics error model of the robot. The proposed calibration approach is applied on a Katana 450 serial robotic manipulator. The robot is controlled through the MATLAB, and Optotrack system measures absolute full poses of the robot for calibration. The robot is calibrated using both conventional and proposed method to investigate the influence of joint tilting on pose accuracy of the robot.

4.1 Introduction

Serial robotic manipulators have large applications in manufacturing, medical, automobile assembly lines, outer space applications and much more. The errors in geometric parameters such as errors in link length, joint twist, and joint angle offsets, as well as non-geometric factors such as joint and link flexibility, joint clearance due to design and manufacturing tolerances, wear and tear, and gears backlash affect the pose (i.e. positional and orientation) accuracy of serial robots (Mooring et al., 1991). The geometric parameters errors can now be systematically identified and compensated whereas non-geometric errors such as joints tilting, and joints deflection

are still difficult to model and identify. The main reason that causes the pose error is inaccurate geometric parameters used to calculate the pose. Hence conventional kinematics calibration fulfils the desired pose accuracy for many applications (Shiakolas et al., 2002). However, some of the applications demand higher positioning accuracy of a robot, and hence the errors due to non-geometric factors must be identified and compensated to achieve desired pose accuracy (Chen-Gang et al., 2014). For example, laser cutting of stamped steel in the automobile industry and drilling of thousands of holes on aircraft wings, where the robot is programmed off -line and tolerances are tight.

Several types of research have been conducted for the calibration of serial robotic manipulators considering geometric and non-geometric errors. (Caenen and Angue, 1990, Gong et al., 2000, Jang et al., 2001, Khalil and Besnard, 2002, Tao et al., 2012, Jawale and Thorat, 2013, Klimchik et al., 2013, Angelidis and Vosniakos, 2014, Zhou et al., 2014, Joubair and Bonev, 2015). Caenen and Angue (1990) and Gong et al. (2000) identify and compensate for the axial component of joint stiffness on top of the errors in geometric parameters of the robot. However, the simultaneous identification of geometric error and joints stiffness has not been explained clearly. Indeed, pose errors due to joints stiffness, i.e. one of the non-geometric errors, must be corrected before approximation of geometric errors. Khalil and Besnard (2002) customise the Newton Euler method to calculate the forces and moments acting at the links and joints to estimate the deformations of links and joints. However, this research ignores the pose errors due to joint clearance and backlash at the joints. Jawale and Thorat (2013) estimated positional errors of serial robot end-effector considering the joint clearances and backlash. However, the simulations are carried out assuming stiff joints and links and ignores the pose errors due to joints and links flexibility. Jang et al. (2001) divides the workspace into the small regions and uses Radial Basis Function Network (RBFN) to approximate the flexibility of joint as a function of workspace position. However, as the influence of joint errors is different at every single position, and hence its inverse approximation regarding workspace coordinates cannot be accurate. Angelidis and Vosniakos (2014) use Artificial Neural Network (ANN) to compensate end-effectors errors without changing actual kinematics model. However, this approach is not effective because joint angles are changed to compensate for the geometric and non-geometric errors for a specific trajectory only. Zhou et al. (2014) presented an algorithm for simultaneous identification of kinematics parameters errors and

positional errors due to axial compliance. However, their research ignores joint errors due backlash and joint clearance. Joubair and Bonev (2015) apply planar constraints to obtain kinematics and stiffness parameters. However, error in all pentameters could not be identified with their proposed approach. All previous researchers have

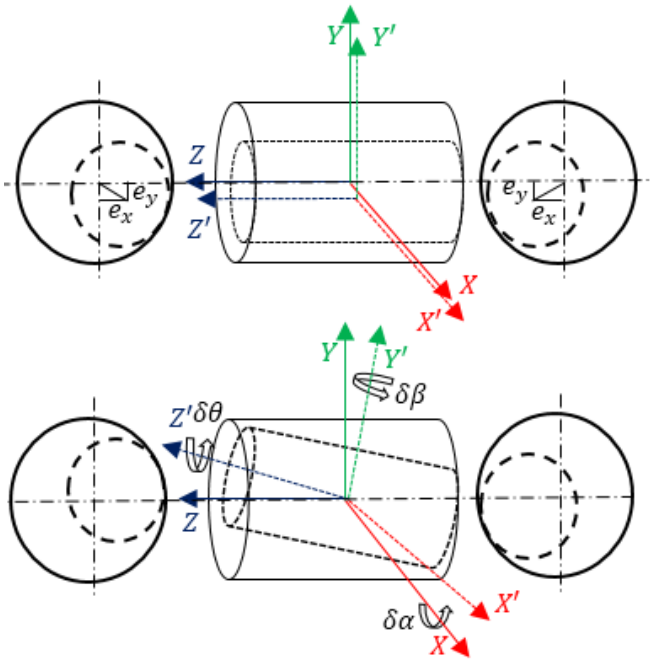

Fig. 4.1 Spindle eccentric errors (upper) and spindle tilt errors (lower)

considerably improved pose accuracy of the serial robot by considering the effect of joints flexibility (i.e. axial compliance) on top of the geometric parameters errors.

However, the joint tilting due to the combined effect of joint clearance and backlash has not been carefully addressed for the calibration of serial robots by previous researchers. The joint errors should be divided into constant geometric parameters errors (i.e. joint twist error, encoders offsets) and variable error due to non-geometric factors (i.e. error due to joint clearance, backlash, joint flexibility, etc.) leading to joint tilting. The magnitude and orientation of a joint tilting also depend on the configuration, and static forces and moments acting at that joint. Modelling the tilting behaviour of a joint can be difficult due to its dependency on some factors. For example, the joint clearance introduces eccentric errors e_x and e_y as shown in Fig. 4.1. Effect of these linear joint errors has minute effect on the robot tool pose. However, the same joint clearance can also contribute to the joint tilting that can be described as three rotational errors δ_α, δ_β and δ_θ as shown in Fig. 4.1. Due to the nature of coupling of the links in serial manipulators, even small joint tilting can cause larger pose error

at the robot end-effectors. In serial manipulators, maximum errors originated at the joints propagate and amplify towards the end-effector of a robot. Error in the length of a link causes same positional error over the entire workspace of the robot, whereas the joint parameters errors have configuration dependent influence on the pose accuracy of the robot. For example, the positional error at point P_1would be larger compare to the positional error, illustrated in Fig. 4.2, at the point P_2 for an error of a degree in θ_1. However, an error of tenth of a millimeter in a_1 leads to same positional error at P_1 and P_2 and no orientation errors at all. The identification of geometric parameters errors and joint stiffness can be incorrect if joint tilting is not considered, and hence the positioning accuracy cannot be improved after a certain level. Therefore, to address this issue, this research models the joint tilting as a resultant effect of axial joint compliance, eccentric and backlash errors. Due to the scope of investigation and minor

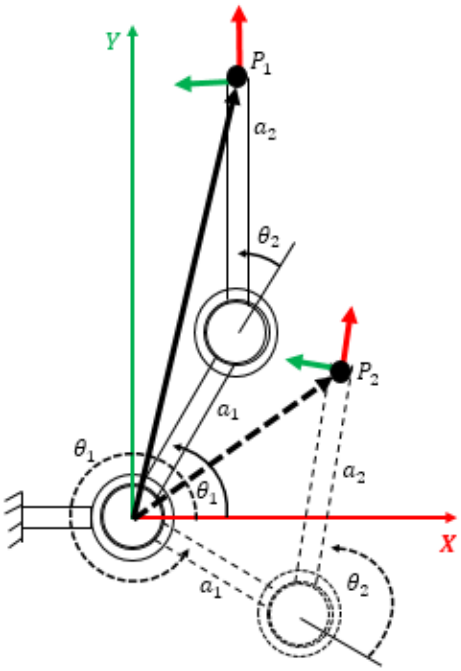

Fig. 4.2 Influence of error on robot tool pose

impact on the overall positioning accuracy, this research ignores errors in the links' length of the robot assuming them perfect and rigid, and identifies the errors at the joints only. The actual joint parameters would be compensated with kinematics errors and tilting at each joint. Therefore, at least three rotational parameters would be required to make up for the deviation of joint orientation due to kinematics errors (i.e. error in a joint twist and joint offset) as well as tilting. Hence, Section 4.2 modifies the kinematics model of the robot used for this research to facilitate three rotational

parameters at each joint without increasing redundancy, Section 4.3 prepares error model, Section 4.4 explains error identification, Section 4.5 performs the experiments to compare the proposed approach against conventional method, and Section 4.6 concludes the research.

4.2 Kinematics modelling of Katana 450 robot

The kinematics model of the robot establishes a relationship between joint link parameters and end-effectors pose of a robot. Different researchers (Hayati and Mirmirani, 1985, Zhuang et al., 1990, Zhuang et al., 1993, Craig, 2005, Tao et al., 2012) have proposed several kinematics modelling methods. In the original DH method, the coordinate system and parameters are defined strictly. However, in the original DH method, the orientation of the base coordinate system is related to the first joint which restricts the assignment of base coordinates. The modified DH method uses new transformation to facilitate the arbitrary frame assignment for the base coordinate (Craig, 2005). However, when the adjacent joint axes are parallel, the little tilting causes a dramatic change in parameters leading to discontinuity of the

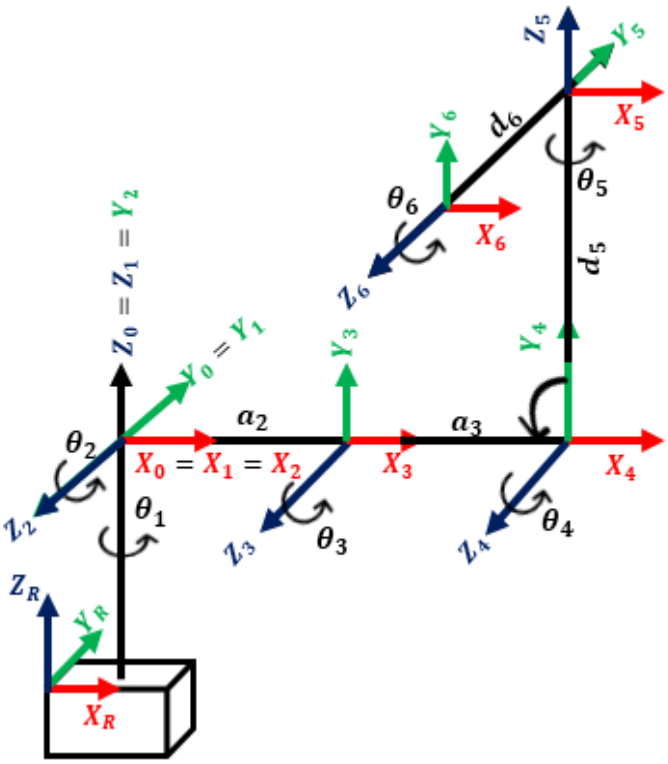

Fig. 4.3 Frames assignment

kinematics model. The improved DH method adds a parameter in the link transformation, which is used to avoid discontinuity (Hayati and Mirmirani, 1985).

However, the introduction of additional parameters also increases the redundancy, which requires additional parameters handling (Meggiolaro and Dubowsky, 2000). The modified DH method is still widely used for the kinematic modelling of industrial robots, and employed by controllers of robots. This research modifies the kinematic model of the Katana 450 robot which is based on the modified DH method. From the specifications of the Katana 450 robot, the nominal values of the kinematics parameters are listed in Table 4.1 as per modified DH method used by the robot controller. Some changes have been made to the actual kinematics model of the robot. The joint six is kept inactive in this research and hence does not influence the pose of the robot. The 118-mm long robot gripper is replaced by a custom designed 200 mm long link, and hence the frame {6} as shown in Fig. 4.3 is considered as the tool frame.

Table 4.1 Kinematics parameters of Katana 450

Joint i	$\alpha_{i-1}{}^{o}$	a_{i-1} *mm*	$\theta_i{}^{o}$	$\beta_{i-1}{}^{o}$	d_i *mm*
1	0	0	+/-169.5	-	0
2	90	0	+102 / -30	-	0
3	0	190	+/-122.5	0	-
4	0	139	+/-112	0	-
5	-90	0	+/-168	0	147.3
6	90	0	Inactive	0	200

The base coordinate frame {0} in the robot controller is at the intersection of first two joints, which is different from the structural base of the robot as shown in Fig. 4.3. Therefore, a digitising probe is used to mark the reference coordinates frame{R}, and the Optotrack can directly measure the tool frame {6} on the reference coordinates frame {R}. In the modified DH method (Craig, 2005), the frame i is rigidly attached to the link i, which rotates around joint i. The transformations ${}^{i-1}_{i}T$ between the frames $(i-1)$ and i is described with the help of two rotational parameters, i.e. joint twist α_{i-1} and joint angle θ_i, and two translational parameters, i.e. link length a_{i-1} and link offset d_i. Therefore, the homogeneous link transformation matrix ${}^{i-1}_{i}T$ in is calculated as:

$$ {}^{i-1}_{i}T = Rot(X,\alpha_{i-1})Trans(X,a_{i-1})Rot(Z,\theta_i)Trans(Z,d_i). \qquad (4.1) $$

However, three rotational parameters are required to present joint orientation while considering joint as shown in Fig. 4.1. The base frame of the robot is at the intersection

of joint 1 and joint 2, and there is no link length or link offset present between the base frame {0} and frame {3} as shown in Fig. 4.3. Therefore, the combined transformations of θ_1, α_2, θ_2 and α_2 is sufficient to describe frame {3} on frame {0}, and to incorporate kinematics errors and tilting. All other parameters are eliminated from Table 4.1 Kinematics parameters of Katana 450 to avoid redundancy (Meggiolaro and Dubowsky, 2000), and the transformation matrix $\mathbf{{}^0_3T}$ is calculated as:

$$\mathbf{{}^0_3T} = Rot(Z,\theta_1)Rot(X,\alpha_2)Rot(Z,\theta_2)Tran(X,190) \tag{4.2}$$

An additional parameter β is used to retain the continuity of the kinematic model as suggested in improved DH method (Hayati and Mirmirani, 1985). Therefore, to facilitate three rotations at the same joint, transformation matrices ${}^3_4T$, ${}^4_5T$, and ${}^5_6T$ are described as:

$${}^3_4T = Rot(X,\alpha_3)Rot(Y,\beta_3)Rot(Z,\theta_3)Tran(X,139)\,, \tag{4.3}$$

$${}^4_5T = Rot(Z,\theta_4)Rot(Y,\beta_4)Rot(X,\alpha_4 = -90)Tran(Z,147.3), \tag{4.4}$$

$${}^5_6T = Rot(Z,\theta_5)Rot(Y,\beta_5)Rot(X,\alpha_5 = 90)Tran(Z,200). \tag{4.5}$$

Finally, the pose of robot end-effector frame {6} on base frame {0} can be described using the transformation ${}^0_6T$ as:

$${}^0_6T = \mathbf{{}^0_3T} \cdot {}^3_4T \cdot {}^4_5T \cdot {}^5_6T. \tag{4.6}$$

The measurement system will measure the robot end-effector pose as:

$${}^R_6T = {}^R_0T \cdot {}^0_6T, \tag{4.7}$$

where the translation transformation ${}^R_0T = [55\ 55\ 201.5]'\,mm$ is from the design specifications of the Katana 450 robot. The homogeneous transformation matrix ${}^0_6T$ in (4.6) describes the position and orientation of the robot end-effectors with respect to the robot's nominal base. Forward kinematics model in (4.6) was verified against robot control software. The reachable workspace of the robot can be found using forward kinematics model, and the joint angle ranges in Table 4.1. The kinematics model of the Katana 450 robot uses ZXZ Euler angle method to describe the orientation of robot's end-effector as angles Φ, θ, and Ψ. Therefore, the pose P of robot is defined by the coordinates X, Y, and Z and orientation angles Φ, θ, and Ψ in form of vector $P = [X\ \ Y\ \ Z\ \Phi\ \theta\ \ \Psi]^T$.

4.3 Error model

For the calibration purpose, the positional error ΔP between the actual position P_{actual} and the theoretical position P_{theor} of the end-effectors is described as:

$$\Delta P = P_{actual} - P_{theor} = [\Delta X \ \ \Delta Y \ \ \Delta Z]^T. \tag{4.8}$$

Positional errors are sufficient to identify errors in the joint-link parameters of a serial robotic manipulator (Klimchik et al., 2013). Therefore, orientation errors $\Delta\Phi,\ \Delta\theta,\ and\ \Delta\Psi$ are not considered during the errors identification, however, measured before and after the calibration at each position. There are three rotational parameters in each of the transformations ${}^{0}_{3}T$, ${}^{3}_{4}T$, ${}^{4}_{5}T$, and ${}^{5}_{6}T$ to compensate the components of joint errors $\Delta\alpha, \Delta\beta$ and $\Delta\theta$ (θ_1, α_1, and θ_2 in ${}^{0}_{2}T$). The joint errors for the joint i can be modelled as:

$$\begin{bmatrix}\Delta\alpha_i \\ \Delta\beta_i \\ \Delta\theta_i\end{bmatrix} = \begin{bmatrix}\Delta\alpha_i^{twist} \\ \Delta\beta_i^{twist} \\ \Delta\theta_i^{offset}\end{bmatrix} + \begin{bmatrix}\delta\alpha_i \\ \delta\beta_i \\ \delta\theta_i\end{bmatrix}, \tag{4.9}$$

where, $\Delta\alpha_i^{twist}$and $\Delta\beta_i^{twist}$are errors in joint twist (i.e. also called kinematics or geometric errors), and $\Delta\theta_i^{offset}$is encoder's offset, whereas $\delta\alpha_i, \delta\beta_i,$ and $\delta\theta_i$ are three components of joint tilting which is defined as:

$$\begin{bmatrix}\delta\alpha_i \\ \delta\beta_i \\ \delta\theta_i\end{bmatrix} = \begin{bmatrix}\delta\alpha_i^{cle} \\ \delta\beta_i^{cle} \\ \delta\theta_i^{bkl}\end{bmatrix} + \begin{bmatrix}0 \\ 0 \\ \delta\theta_i^{axic}\end{bmatrix}, \tag{4.10}$$

where, $\delta\alpha_i^{cle}$,$\delta\beta_i^{cle}$, and $\delta\theta_i^{bkl}$ are components of joint tilting due to joint clearance and backlash, and $\delta\theta_i^{axic}$ is component of joint tilting due to joint compliance (i.e. due to joint flexibility). The titling of the joint due to clearances and backlash has fixed magnitude, and the orientation depends upon the moment acting at the joint, The previous works (Zhu and Ting, 2000) models the robotic joints with clearance considering only linear effect of eccentric errors (i.e. $\sqrt{e_x^2 + e_y^2}$ in Fig. 4.4) on end-effectors position, and ignores the joint tilting due to clearance. The another research

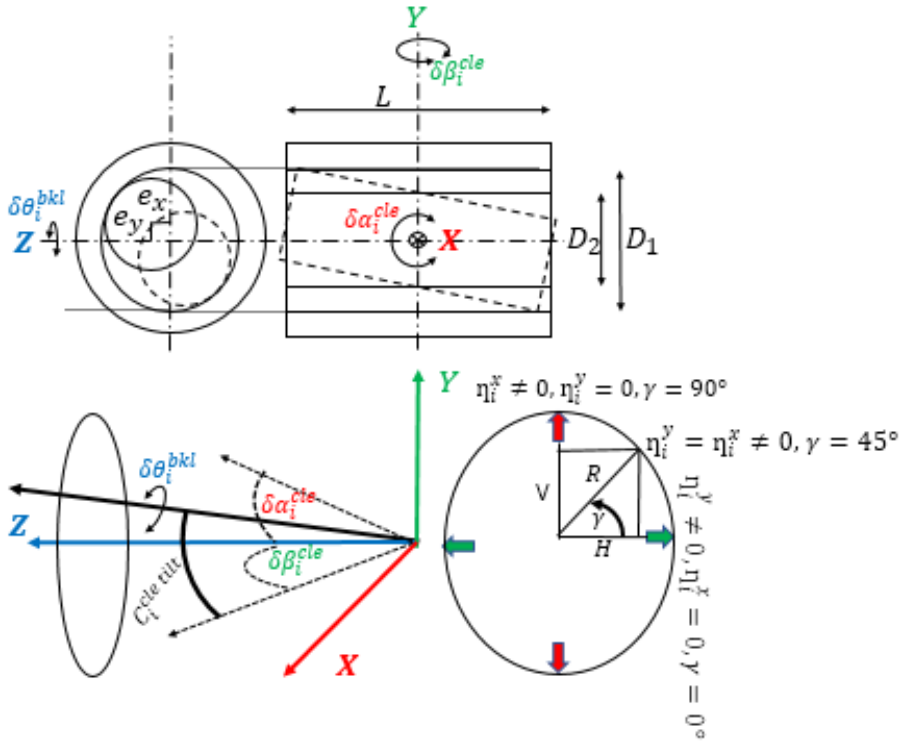

Fig. 4.4 Joint tilting due to clearance and backlash

(Kakizaki et al., 1993) considers joint titling only due to clearance, however, uses two parameters θ and α based on standard DH method to describe joint orientation which are not sufficient to represent joint tilting, because the joint titling can have any orientation depending on the direction and magnitude of moments acting at the joint. Therefore, this research models the tilting of joint as in Fig. 4.4. The joint profile is considered uniform (i.e. $e_x = e_y$ when center axis of pin and housing are in line), and there no linear axial error ($e_z = 0$) present in the joint. The joint clearance is considered very small such that pin has either two-point contact with housing as shown in Fig. 4.4 such that tilting angle $C_i^{cle\ tilt}$ due to clearance as:

$$C_i^{cle\ tilt} = \sin^{-1}\left(\frac{R}{\sqrt{\left(\frac{L}{2}\right)^2 + R^2}}\right), \tag{4.11}$$

where R=$(D_1 - D_2)/2$ or axial contact such that eccentric error would be $\sqrt{e_x^2 + e_y^2}$ and $Rot\left(X, \delta\alpha_i^{cle}\right)Rot\left(Y, \delta\beta_i^{cle}\right) = 0$ (i.e. no joint tilting due to joint clearance). The $\delta\theta_i^{bkl}$ can be directly considered as axial angular error due to backlash. However, the components of $C_i^{cle\ tilt}$ in the form of $\delta\alpha_i^{cle}$ and $\delta\beta_i^{cle}$ must be found from the moments

η_i^x and η_i^y acting at the joint (equation of the moment vector is in section 4). The angle γ can be determined from the proportion of the moments η_i^x and η_i^y acting at the joint as shown in Fig. 4.4. Consider $H = R\cos\gamma$ and $V = R\sin\gamma$ in Fig. 4.4, then $\delta\alpha_i^{cle}$, $\delta\beta_i^{cle}$ and $\delta\theta_i^{bkl}$ in (4.10) can be calculated as:

$$\delta\alpha_i^{cle} = \frac{V}{\sqrt{\left(L/2\right)^2 + V^2}},\ \delta\beta_i^{cle} = \frac{H}{\sqrt{\left(L/2\right)^2 + H^2}},\ \delta\theta_i^{bkl} = backlash°. \tag{4.12}$$

Therefore, joint tilting (i.e. change in the orientation of a joint) due to clearance and backlash can be defined by the transformations:

$$Rot(X, \delta\alpha_i^{cle})Rot(Y, \delta\beta_i^{cle})\ Rot(Z, \delta\theta_i^{bkl}). \tag{4.13}$$

The Cartesian positional error ΔP_{cb} due to joints tilting because of joints clearance and backlash can be calculated using the identification Jacobean as:

$$\Delta P_{cb} = J.\Delta E^{cb}, \tag{4.14}$$

where, $\Delta E^{cb} = [\delta\theta_{1\ldots}^{bkl}\delta\theta_5^{bkl}\ \delta\alpha_{1\ldots}^{cle}\delta\alpha_5^{cle}\ \ \delta\beta_{2\ldots}^{cle}\delta\beta_5^{cle}\ ]^T$,

and the Jacobin $J = \begin{bmatrix} \frac{\partial P_X}{\partial\theta_1}..\frac{\partial P_X}{\partial\theta_5} & \frac{\partial P_X}{\partial\alpha_1}..\frac{\partial P_X}{\partial\alpha_5} & \frac{\partial P_X}{\partial\beta_2}..\frac{\partial P_X}{\partial\beta_5} \\ \frac{\partial P_Y}{\partial\theta_1}..\frac{\partial P_Y}{\partial\theta_5} & \frac{\partial P_Y}{\partial\alpha_1}..\frac{\partial P_Y}{\partial\alpha_5} & \frac{\partial P_Y}{\partial\beta_2}..\frac{\partial P_Y}{\partial\beta_5} \\ \frac{\partial P_Z}{\partial\theta_1}..\frac{\partial P_Z}{\partial\theta_5} & \frac{\partial P_Z}{\partial\alpha_1}..\frac{\partial P_Z}{\partial\alpha_5} & \frac{\partial P_Z}{\partial\beta_2}..\frac{\partial P_Z}{\partial\beta_5} \end{bmatrix}$.

Joint flexibility (i.e. joint compliance) is another factor which also causes joint tilting. Joint tilting because of joint flexibility depends on joint stiffness, and the direction as well as the magnitude of moments acting at the joint. Due to the cylindrical geometry of the revolute joint in robot manipulator, it has axial compliance $C_i^{axi\ comp}$ and radial compliance $C_i^{rad\ comp}$. The axial compliance (i.e. about the axis of revolution) is much larger compare to the radial compliance as joint is supported radially by bearings. Therefore, the earlier research (Zhou et al., 2014) ignores the joint deflections due to radial compliance. If the robot joint is modeled as a linear torsional spring, the components of tilting $\delta\theta_i^{axic}$ (i.e. joint deflection due to axial compliance) in (4.10) can be obtained as:

$$\begin{bmatrix} 0 \\ 0 \\ \delta\theta_i^{axic} \end{bmatrix} = \begin{bmatrix} 0 \\ 0 \\ \eta_i^z / k_i^z \end{bmatrix} = \begin{bmatrix} 0 \\ 0 \\ \eta_z C_i^{axi\ comp} \end{bmatrix}, \tag{4.15}$$

where, η_i^z is the moment acting about Z axis of the joint i. The Cartesian positional error $\Delta P_{compliance}$ because of joints deflection can be calculated as:

$$\Delta P_{compliance} = J.\Delta E^{compliance}, \tag{4.16}$$

where, $\Delta E^{compliance} = [\delta\theta_1^{axic}\ \delta\theta_2^{axic}\ \delta\theta_3^{axic}\ \delta\theta_4^{axic}\delta\theta_5^{axic}\ ]^T$.

Finally, the Cartesian positional error ΔP_{geom} due to small joint twist and joint offset are calculated using the identification Jacobean as:

$$\Delta P_{geom} = J.\Delta E^{geom}, \tag{4.17}$$

where, $\Delta E^{geom} = [\Delta\theta_{1....}^{offset}\Delta\theta_5^{offset}\ \Delta\alpha_{1...}^{twist}\Delta\alpha_4^{twist}\ \Delta\beta_{2...}^{twist}\Delta\beta_5^{twist}\ ]^T$.

Considering the Cartesian errors ΔP_{geom}, ΔP_{cb} and $\Delta P_{compliance}$, the actual position of robot end-effector, P_{actual} is defined as:

$$P_{actual} = P_{theor} + \Delta P_{geom} + \Delta P_{cb} + \Delta P_{compliance} + \Delta P_{other} \tag{4.18}$$

Where, ΔP_{other} is Cartesian error due to the factors such as temperature, friction, control loop error, noise etc., which are ignored in this research. Hence the actual position of the robot end-effector is defined as:

$$P_{actual} = P_{theor} + \Delta P_{geom} + \Delta P_{cb} + \Delta P_{compliance} \tag{4.19}$$

From (4.8) and (4.19), the positional error can be defined as:

$$\Delta P = \Delta P_{geom} + \Delta P_{cb} + \Delta P_{compliance} \tag{4.20}$$

The following section would explain the identification of joint errors that contribute to the positional errors in (4.20).

4.4 Error identification

4.4.1 Joint tilting due to clearance, backlash and flexibility

The external forces on the robot's end-effector as well the self-weight of the links induce moments at joints. Each joint tilts in the direction of the moments acting at the joint due to the clearance, backlash and flexibility of joints. Forces and moments acting on link i are depicted in the Fig. 4.5. The frame $\{i\}$ is rigidly attached with the link i. If the static position of the manipulator is considered, the forces and moments acting on the link i are resisted by the joint bearings, except about the axis of joint revolution,

which is balanced by joint torque. The moments acting at the joints of the links can be calculated recursively from end-effectors towards the base. If ${}^{i+1}_{i}R$ is the rotational transformation between the frame$\{i\}$ and frame$\{i+1\}$, $[r_i]_i$ is the positional vector from frame$\{i\}$ to frame$\{\ i+1\}$, $[s_i]_i$ is vector from frame $\{i\}$ to the center of gravity of link i, and $[F_{i+1}]_{i+1}$ and $[\eta_{i+1}]_{i+1}$are the vectors of forces and moments acting on the frame $\{\ i+1\}$ respectively, then three dimensional vector of moments $[\eta_i]_i$ at the joint i can be calculate as:

$$[\eta_i]_i = {}^{i+1}_{i}R[\eta_{i+1}]_{i+1} + [r_i]_i \times [F_{i+1}]_{i+1} + [s_i]_i \times m_i\, {}^{0}_{i}R^T[g]_0. \qquad (4.21)$$

The moment vector $[\eta_i]_i = [\eta_i^x\ \eta_i^y\ \eta_i^z\ ]^{\mathrm{T}}$ at joint i can be calculate using (4.21) and parameters in the Table 4.2 for various configurations. The magnitude and direction of moments helps to determine the configurations to separate joint tilting due to the joint clearance and backlash, and joint tilting due the joint flexibility. One of the example configuration is shown in Fig. 4.6. The setup in Fig. 4.6 directly measures the joint tilting errors with the help of inclinometers with the resolution of 0.001° for a specific pose.

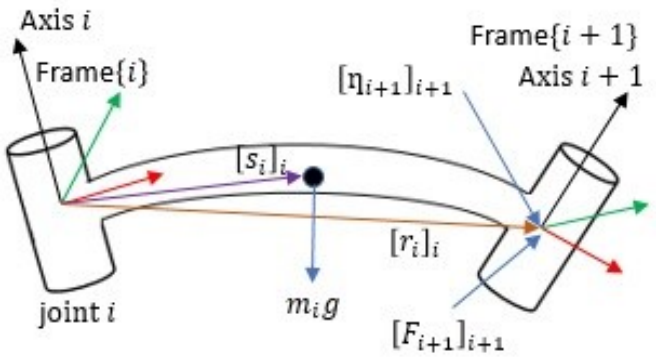

Fig. 4.5 Forces and moments acting on the link i

Table 4.2 Katana 450 Specifications

Parameters of Link i	2	3	4	5
Link length $[r_i]_i$(mm)	190	139	147.3	200
Mass m_i(Kg)	1.03	0.9	1	0.8
COG $[s_i]_i$ (mm)	100	104	80	70

The robot is mounted on the calibration table such the structural base of the robot is properly settled. In this configuration, the last link is rotated about the Z_5 axis (i.e. by changing θ_5) such that end link incline on either sides from the vertical position by 5° , i.e. from -5° to +5°. The relative change in the actual orientation during the rotation on the either side of the 0° is used to measure joints tilting (i.e. $C_2^{cle\ tilt}, C_3^{cle\ tilt}, C_4^{cle\ tilt}$) about X_2, X_2, X_4 axis due to the joints clearance. Note that the readings of the inclinometers encapsulate the elastic deformations of joints. However, due to very high radial stiffness of joints, there would be nearly no joints deformation about X_1, X_2, X_3, and X_4 axis due to the rotation of -5° to +5° about Z_5 axis in this configuration. The inclinometers are used to measure the relative change of orientation between the links as well as first and last link in this configuration. The a relative change in orientation is not affected by the geometric errors (i.e. joint twist error, encoder's offsets). The procedure is repeated for various configuration to identify joint tilting parameters in Table 4.3 associated with clearance and backlash.

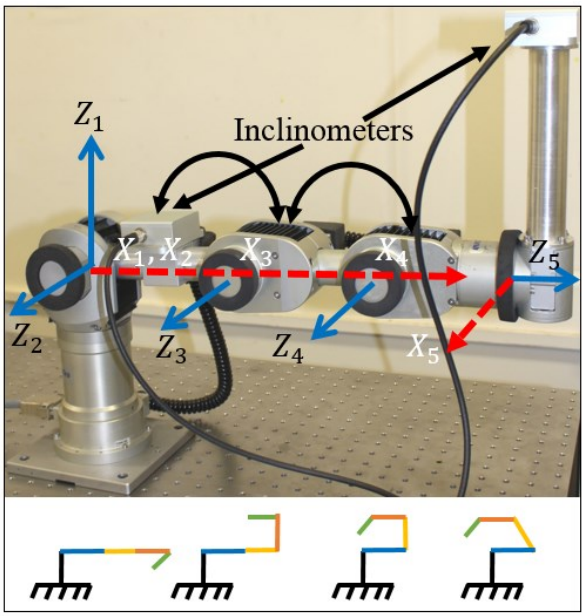

Fig. 4.6 Measurement of joint tilting using inclinometers

Similarly, other configurtions are selected to minimise and maximise the moment about each joint one by one as shown at the bottom of Fig. 4.6. Joints stiffness values in Table 4.4 are obtained by measuring the relative change of joint angle using inclinometer for the calculated change of moment using (4.21). For the identification of $\delta\theta_1^{bkl\circ}$ and k_1^z (which are related to first vertical joint) in Table 4.3 and Table 4.4,

the end-effector pose measurement shown in Fig. 4.8 has been used as (4.21) and inclinometers cannot work without gravity component.

Table 4.3 Parameters related to clearance and backlash

Joint i	1	2	3	4	5
$C_i^{cle\ tilt\circ}$	0.022	0.024	0.017	0.015	0.018
$\delta\theta_i^{bkl\circ}$	0.063	0.061	0.057	0.046	0.051

Table 4.4 Joint stiffness (Kg-m/°)

Joint i	1	2	3	4	5
k_i^z	122	90	75	78	80

4.4.2 Kinematics error identification

Once the joint tilting errors due to clearance and backlash, and compliance are calculated using (4.14) and (4.16) respectively and compensated in (4.20), the Cartesian error ΔP is considered as ΔP_{geom} at a given pose. Errors in geometric parameters are identified using direct pose measurement and well-known least square estimation as:

$$E^{geom} = \frac{J^T}{J \cdot J^T} \cdot \Delta P_{geom} \tag{4.22}$$

In this research, poses have been selected as per proposed performance criteria and related test methods in the ISO 9283:1998 for the robotic manipulators. According to the standard, 118 poses shown in the Fig. 4.8 are chosen on the diagonal planes within the largest cube of the robot's workspace, and some of the poses are selected close to workspace boundary. The measurement is sequenced such that all five joints angles have to be changed when moving from one pose to another. In Fig. 4.8, tails of each point represent the orientation of robot's end-effector, and red, green and blue stripes in the middle indicate X, Y and Z directions of the robot's base frame.

The measurement setup includes a five DOF Katana 450 robot, an Optotrack Certus measurement system from the Northern Digital Inc. with volumetric resolution of 0.01 mm, active vibration isolation table from Thorlabs, and a computer to control the robot

through the serial communication. The 200 mm long and 0.5 Kg customized link shown at the top of Fig. 4.7, act as a payload, amplify the effect of the joint tilting errors due to a larger length, and provide ease of attaching measurement targets. The

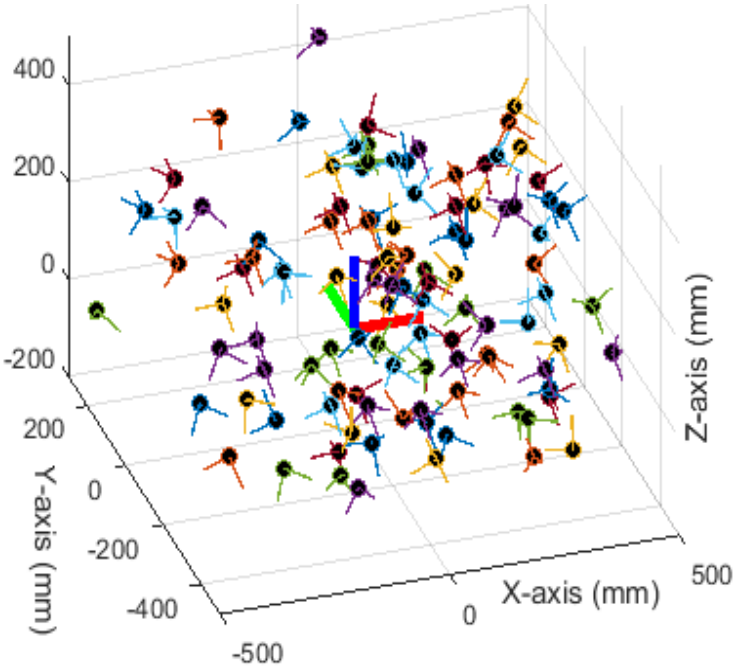

Fig. 4.8 Selection of measurement poses

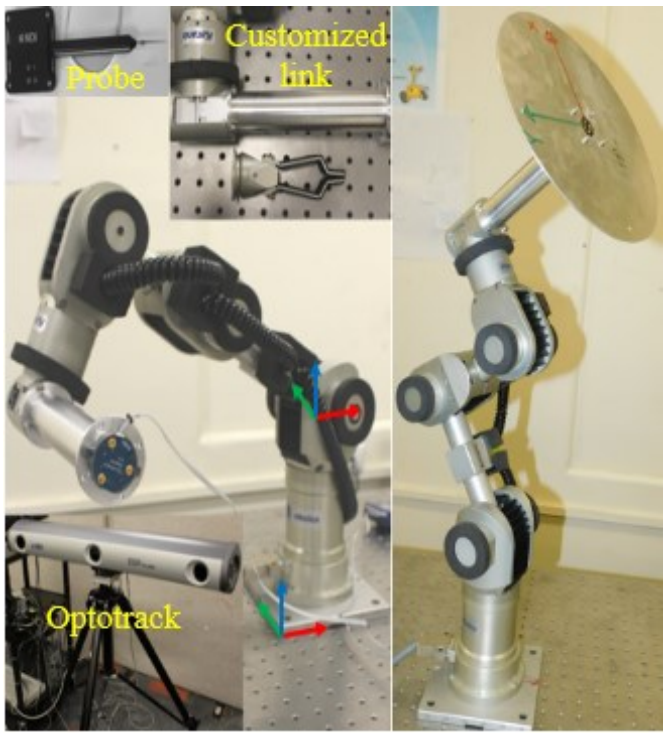

Fig. 4.7 Experimental setup

robot is controlled with the MATLAB using Katana Native Interface language for the calibration, and modification of the kinematic parameters after the calibration. The digitising probe shown in the top-left corner of Fig. 4.7 used to establish the global coordinate system for the measurements. The system measures Cartesian coordinates of three active markers on the established global coordinates system at the structural base of the robot. The coordinates of three markers are used to calculate the position as well as the orientation of the robot's end-effector on the structural base of the robot as shown in Fig. 4.7, which is then transformed into the robot's nominal base using

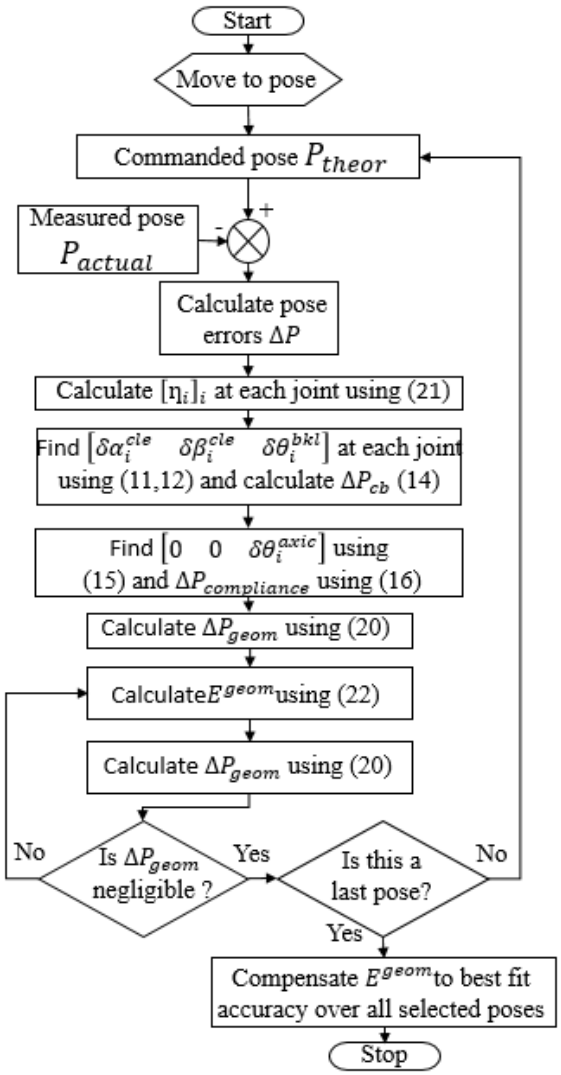

Fig. 4.9 Calibration process

(4.6) and (4.7). Multiple measurement targets have been attached to specifically magnify the orientation errors on the disk shown in the left half on Fig. 4.7. Equation (4.22) is repeatedly used at each pose, and over the selected poses to find a set of

kinematics parameters to best fit accuracy over all selected poses (Chen-Gang et al., 2014). The process of proposed calibration can be depicted as in Fig. 4.9. Note that the proposed calibration process first corrects the pose error due to joints tilting and joints flexibility at each pose before identifying the geometric error in the robot's kinematics parameters. Pose error due to joint joints tilting and joints flexibility vary significantly from one configuration to another. Therefore, their prior compensation minimises the chances of incorrect geometric error identification.

4.5 Experimental results

This Section compares the improvement in the positional accuracy after standard calibration with the proposed approach to investigate the influence of joint tilting. The standard kinematics calibration reduced average positional error from 1.21 mm to 0.33 mm. The consideration of joints tilting reduced error from 0.33 mm to 0.12 mm which is a significant reduction in the error as listed in Table 4.5. The significant improvement in the pose accuracy is found at the uncalibrated points of the robot's workspace as well as in Table 4.6. It is difficult to compare the improvement of pose accuracy regarding percentage with previous research because an error in the geometric parameters are still approximated from the end-effectors poses once the joint tilting is compensated. However, from the results in Table 4.6 for uncalibrated points of the robot workspace, it can be claimed that pose accuracy remains concentrated around 0.12 mm for the robot subject to experiment. This is because configuration dependent joint tilting has been encapsulated during the proposed calibration approach. Opposite to that, the conventional calibration has been found effective for the calibrated points only, and improvement in the pose accuracy found inconsistent for uncalibrated points in the robot's workspace. The research in the past has claimed the improvement in the pose accuracy from few millimetres to even less than a tenth of the millimetre. The results of an intensive experiments in this research indicated that even if the robot kinematics model is compensated for the geometric errors, joint stiffness and joint tilting, the improvement in the positioning accuracy beyond 0.1 mm would depend on other factors such as control, encoders resolution, noise, temperature and mechanism of the robot itself.

Table 4.5 Calibration results (over 118 points)

	Pose parameter	Before the calibration	Conventional calibration	Proposed approach
Minimum	$\|\Delta X\|$	0.04	0.02	0.01
	$\|\Delta Y\|$	0.02	0.01	0.00
	$\|\Delta Z\|$	0.08	0.03	0.02
	$\|\Delta P\|$	0.16	0.05	0.03
	$\|\Delta \Phi\|°$	0.04	0.02	0.02
	$\|\Delta \theta\ \|°$	0.05	0.02	0.02
	$\|\Delta \Psi\|°$	0.03	0.01	0.01
Maximum	$\|\Delta X\|$	1.35	0.28	0.14
	$\|\Delta Y\|$	0.92	0.41	0.13
	$\|\Delta Z\|$	1.82	0.63	0.16
	$\|\Delta P\|$	2.11	0.70	0.24
	$\|\Delta \Phi\|°$	0.46	0.125	0.119
	$\|\Delta \theta\ \|°$	0.26	0.087	0.078
	$\|\Delta \Psi\|°$	0.45	0.130	0.09
Average	$\|\Delta X\|$	0.63	0.17	0.08
	$\|\Delta Y\|$	0.44	0.09	0.05
	$\|\Delta Z\|$	0.85	0.25	0.11
	$\|\Delta P\|$	1.21	0.33	0.12
	$\|\Delta \Phi\|°$	0.27	0.096	0.088
	$\|\Delta \theta\ \|°$	0.17	0.027	0.022
	$\|\Delta \Psi\|°$	0.26	0.084	0.079

Table 4.6 Improvement over uncalibrated points

Pose number	Before the calibration $\|\Delta P\|$	Conventional calibration $\|\Delta P\|$	Proposed approach $\|\Delta P\|$
1	1.16	0.51	0.11
2	0.95	0.67	0.12
3	1.52	0.75	0.14
4	1.31	0.55	0.12
5	0.89	0.53	0.11
6	0.93	0.47	0.14
7	1.17	0.28	0.12
8	1.38	0.72	0.16
9	1.54	0.41	0.15
10	0.76	0.25	0.11

4.6 Conclusion

The modifications of the kinematics model of the robot effectively incorporate joint tilting errors. The proposed approach for modelling of the joint tilting errors has proven to be more effective in improving the pose accuracy of the serial robot than the standard kinematics calibration. From the calibration results, this research concludes that consideration of joints tilting during the calibration significantly enhance the pose accuracy of serial robotic manipulators over the entire workspace including for the uncalibrated points as well. The fluctuation of pose errors over entire workspace of a robot can be significantly reduced by compensating for the joints tilting before the geometric error identification. Proposed approach can be further developed for improving the dynamic pose accuracy of the serial robotic manipulators.

Acknowledgement

We would like to thank the School of Mechanical Engineering, the University of Adelaide for providing resources and assistance in for the research.

CHAPTER 5 JOURNAL PAPER 2

Statement of Authorship

Title of Paper	Calibration of serial robots to improve trajectory tracking accuracy by considering joints tilting using a low-cost measurement method
Publication Status	☐ Published ☐ Accepted for Publication ☑ Submitted for Publication ☐ Unpublished and Unsubmitted work written in manuscript style
Publication Details	PATEL, D., LU, T.-F. & CHEN, L. 2017. Calibration of serial robots to improve trajectory tracking accuracy by considering joints tilting using a low-cost measurement method. *Robotica*.

Principal Author

Name of Principal Author (Candidate)	Dhavalkumar Patel		
Contribution to the Paper	Established concept, derived mathematics, performed experiments, interpreted data, wrote manuscript and acted as corresponding author.		
Overall percentage (%)	60 %		
Certification:	This paper reports on original research I conducted during the period of my Higher Degree by Research candidature and is not subject to any obligations or contractual agreements with a third party that would constrain its inclusion in this thesis. I am the primary author of this paper.		
Signature		Date	21 NOV 2017

Co-Author Contributions

By signing the Statement of Authorship, each author certifies that:

i. the candidate's stated contribution to the publication is accurate (as detailed above);

ii. permission is granted for the candidate in include the publication in the thesis; and

iii. the sum of all co-author contributions is equal to 100% less the candidate's stated contribution.

Name of Co-Author	Tien-Fu Lu		
Contribution to the Paper	Supervised development of work, helped in data interpretation and manuscript evaluation.		
Signature		Date	23/11/2017

Name of Co-Author	Lei Chen		
Contribution to the Paper	Helped to evaluate and edit the manuscript.		
Signature		Date	24/11/17

Title: Calibration of serial robots to enhance trajectory tracking by considering joints tilting and a low-cost measurement method

Dhavalkumar Patel, Tien-Fu Lu and Lei Chen

School of Mechanical Engineering, University of Adelaide, Adelaide 5005, Australia

Keywords: Robot calibration, Errors identification, Joints tilting, Trajectory, Robot kinematics

Abstract

The ability of serial robots to accurately follow a desired trajectory could be profoundly affected by joints tilting because of joint clearance, backlash and joint flexibility. Conventional calibration rectifies geometric errors and compensates for the joints flexibility, which could not improve robot's tracking accuracy above a certain level if joints tilting is ignored during the calibration. Additionally, expensive measurement equipment customarily employed increases the cost of robot calibration. Therefore, this research presents the mathematics required to encapsulate joints tilting to improve the trajectory tracking accuracy of a serial robot as well as a low-cost measurement set-up. Kinematics model of a Katana 450 robot is modified to incorporate joint tilting. The robot is controlled through MATLAB to implement the proposed method. Optotrack system is used to validate both improvements in accuracy and the custom designed measurement setup.

5.1 Introduction

Serial robotic manipulators have numerous applications across various industries. Accurate trajectory tracking is essential for operations such as laser cutting, and robotic surgery performed by serial robotic manipulators. Dynamic pose (i.e. positional and orientation) accuracy of a robot can be far worse than its static pose accuracy. The inaccuracy of the geometric parameters such as link length, link offset, joint twist angle, and joint angle offsets are mainly responsible for the robot's pose errors (Mooring et al., 1991). Therefore, standard geometric calibration fulfils the desired trajectory tracking accuracy for many applications. However, non-geometric factors such as joints flexibility, joint clearance due to design and manufacturing tolerances, wear and tear, and gears backlash can also significantly affect the pose accuracy of serial robots especially when a serial robot is in the motion (Shiakolas et

al., 2002). Kinematics parameters errors can now be systematically detected and compensated whereas non-geometric errors are still difficult to incorporate in the robot calibration.

There are various kinematics modelling methods proposed to build complete and continuous kinematics model of serial robots (Chen-Gang et al., 2014). However, very few research address effects of non-geometric factors such as joint clearance, backlash and joint flexibility. Earlier researchers considered linear errors due to joint clearance and backlash, and do not consider joints tilting due to the small rotation of joint's pin inside the housing (Kakizaki et al., 1993, Zhu and Ting, 2000, Jawale and Thorat, 2013). Joints stiffness can now be identified (Zhou et al., 2014) or approximated over different regions of workspace (Jang et al., 2001). However, none of the research encapsulates the joints tilting which is the combined effect of joint clearance, joints flexibility and backlash. Some of the previous researchers (Zhao et al., 2015, Angelidis and Vosniakos, 2014) indicated the effectiveness of AI techniques for estimation of Cartesian errors and errors compensation through joint angles correction for following particular trajectory.

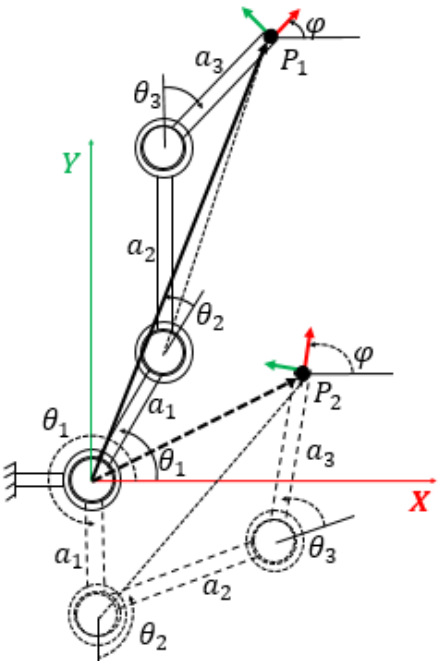

Fig. 5.1 Configuration dependent influence of joint errors

However, a robot calibrated to track a specific trajectory is normally not able to follow a different trajectory with the same accuracy. Even the accuracy may be worse than before the calibration for the different trajectory or in the other region of the robot's

workspace. Due to the nature of the couplings of the links, standard geometric parameter based calibration of serial manipulators suffers from two specific problems. Firstly, an error in the joint parameters such as θ_1, θ_2, and θ_3 have a posture dependent influence on the robot end-effector. For example, error in θ_1 will cause larger error at P_1 in comparison with the same errors of θ_2 as shown in Fig. 5.1. However, it would be exactly opposite in case of P_2. As the conventional calibration identifies the kinematics parameters errors from few data points in the workspace, the error identification may be incorrect in case of mutually dependent joint parameters. Secondly, the combination of joints clearance, backlash and joint flexibility results

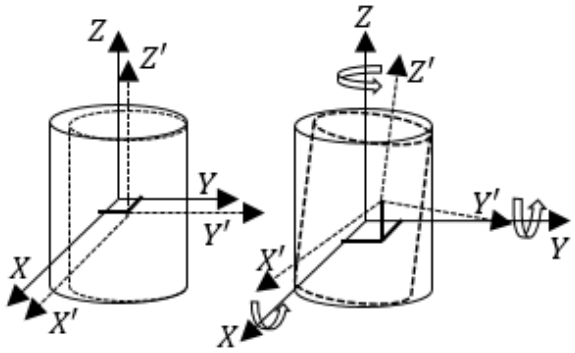

Fig. 5.2 Joint tilting under clearance, backlash, and stiffness

into the joints tilting as shown in Fig. 5.2. The orientation of joints tilting depends on the instantaneous moments acting at the joint when robot is in the motion. The combination of incorrect kinematics joint parameters and joint titling harshly affect the robot accuracy specifically when robot is in the motion. The conventional kinematics calibration will most likely incorrectly modify the joint parameters to best fit the calibration data collected for a specific trajectory if the joint tilting is not considered before the errors identification, and may cause larger errors for a different trajectory because of the configuration dependent influence (Patel et al., 2017) as explained in Fig. 5.1. Hence, this research focuses on the joint errors but assuming perfect links. Moreover, the contemporary measurement technologies such as Optical CMM and Laser trackers increase the cost of robot calibration (Nubiola et al., 2013, Nubiola and Bonev, 2013, Liu et al., 2009). On the other hand, previously proposed low-cost techniques such as Telescoping ball-bar (Nubiola et al., 2013), physical constraint (Ge et al., 2014), Position Sensitive Device (Liu et al., 2009), IMU's (Cantelli et al., 2015), and projection methods (Park and Kim, 2011) are either not suitable for the measurement of a trajectory or requires too much human intervention.

Therefore, this research proposes the mathematics required to encapsulate the joints tilting to further improve trajectory tracking accuracy than conventional geometric parameter based approach, and validates the improvement in accuracy with the help of a low-cost measurement set-up. The remainder of this research paper is organized as follows. Section 5.2 modifies the kinematic model of a robot to present arbitrary orientation of a robot joint. Section 5.3 identifies various joints parameters and explains joint tilting model. Section 5.4 simulates the effect of joints tilting considering the joint clearance, backlash and stiffness. Section 5.5 validates the effectiveness of proposed approach with the high-end measurement device and presents low-cost measurement alternative.

5.2 Kinematics and error model

Kinematics model of the Katana 450 robot follows a modified DH method which is manifested to facilitate three rotational parameters at each joint. Table 5.1 enlists the nominal values of kinematics parameters of the Katana 450 robot.

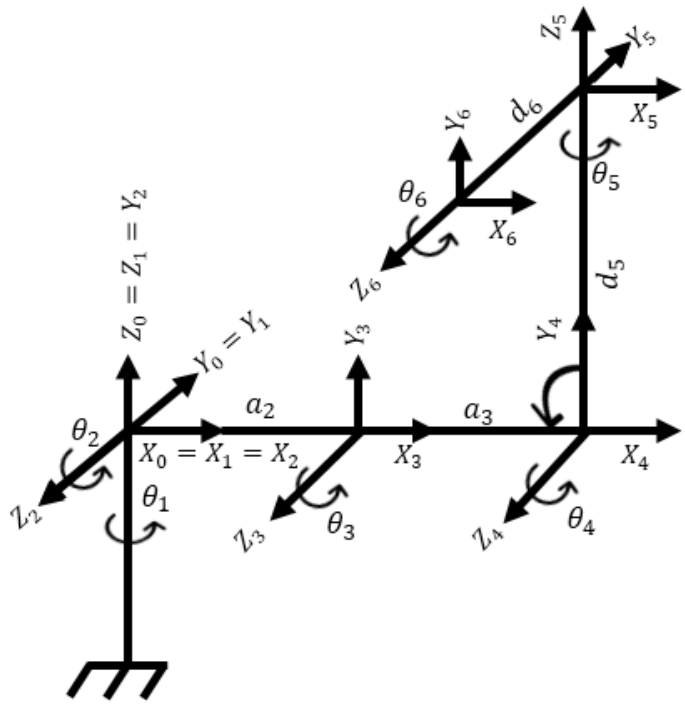

Fig. 5.3 Frames assignment for Katana 450 robot

Table 5.1 Kinematics parameters of Katana 450

Joint i	$\alpha_{i-1}{}^{o}$	a_{i-1} *mm*	$\theta_i{}^{o}$	$\beta_{i-1}{}^{o}$	d_i *mm*
1	0	0	+/-169.5	-	0
2	90	0	+102 / -30	-	0
3	0	190	+/-122.5	-	-
4	0	139	+/-112	0	-
5	-90	0	+/-168	0	147.3
6	90	0	Inactive	0	200 +130

As the Z -axis of joint 1 and joint 2 are intersecting as shown in Fig. 5.3, the transformation matrix between the frame {0} and frame {3} can be derived as:

$$ {}^{0}_{3}T = Rot(Z,\theta_1)Rot(X,\alpha_2)Rot(Z,\theta_2)Tran(X,190) \tag{5.1} $$

An additional parameter β can be used for the continuity of the kinematic model (Hayati and Mirmirani, 1985) and to facilitate three rotations at each joint. Hence, transformation between the frames {3}, {4}, {5}, and {6} can be defined as:

$$ {}^{3}_{4}T = Rot(X,\alpha_3)Rot(Y,\beta_3)Rot(Z,\theta_3)Tran(X,139), \tag{5.2} $$

$$ {}^{4}_{5}T = Rot(Z,\theta_4)Rot(Y,\beta_4)Rot(X,\alpha_4)Tran(Z,147.3)\,, \tag{5.3} $$

$$ {}^{5}_{6}T = Rot(Z,\theta_5)Rot(Y,\beta_5)Rot(X,\alpha_5)Tran(Z,200). \tag{5.4} $$

By multiplying the transformations in (5.1), (5.2), (5.3), and (5.4), the pose of robot end-effector frame {6} with respect to frame {0} can be described using the transformation ${}^{0}_{6}T$ as:

$$ {}^{0}_{6}T = {}^{0}_{3}T \cdot {}^{3}_{4}T \cdot {}^{4}_{5}T \cdot {}^{5}_{6}T. \tag{5.5} $$

The transformation matrix ${}^{0}_{6}T$ in (5.5) describes the pose of the robot end-effectors on the robot's nominal base. Forward kinematics model in (5.6) was verified against robot control software. The reference coordinate system is established at the robot's physical base due to convenience. A translation transformation ${}^{R}_{0}T = [55\ 55\ 201.5]'\ mm$ relates nominal and physical base of the Katana 450 robot. Therefore, the measurement system measures the robot end-effector pose as:

$$ {}^{R}_{6}T = {}^{R}_{0}T \cdot {}^{0}_{6}T. \tag{5.6} $$

Katana 450 robot employs ZXZ Euler angle method to describe orientation of the robot end-effector. Coordinates X, Y, and Z and orientation angles Φ, θ, and Ψ describe the

robot's pose in form of vector $P = [X\ \ Y\ \ Z\ \Phi\ \theta\ \ \Psi]^T$. Positional errors are sufficient to identify errors in the joint-link parameters of a serial robotic manipulator (Klimchik et al., 2013). Therefore, orientation errors $\Delta\Phi,\ \Delta\theta,\ and\ \Delta\Psi$ are not considered during the errors identification. During a calibration, the positional error ΔP between the actual position P_{actual} and the theoretical position P_{theor} of the end-effectors is described as:

$$\Delta P = P_{actual} - P_{theor} = [\Delta X\ \ \Delta Y\ \ \Delta Z]^T. \tag{5.7}$$

There are three rotational parameters in each of the transformations ${}^0_3T$, ${}^3_4T$, ${}^4_5T$, and ${}^5_6T$ to compensate the components of joint errors $\Delta\alpha, \Delta\beta$ and $\Delta\theta$ (Note: three components would be $\Delta\theta_1$, $\Delta\alpha_2$, and $\Delta\theta_2$ in ${}^0_3T$). The joint errors for the joint i can be modeled as:

$$\begin{bmatrix}\Delta\alpha_i\\ \Delta\beta_i\\ \Delta\theta_i\end{bmatrix} = \begin{bmatrix}\Delta\alpha_i^{twist}\\ \Delta\beta_i^{twist}\\ \Delta\theta_i^{offset}\end{bmatrix} + \begin{bmatrix}\delta\alpha_i\\ \delta\beta_i\\ \delta\theta_i\end{bmatrix}, \tag{5.8}$$

where, $\Delta\alpha_i^{twist}$and $\Delta\beta_i^{twist}$are errors in joint twist (i.e. also called kinematics or geometric errors), and $\Delta\theta_i^{offset}$is encoder's offset, whereas $\delta\alpha_i, \delta\beta_i$, and $\delta\theta_i$ are three components of joint tilting which can be defined as:

$$\begin{bmatrix}\delta\alpha_i\\ \delta\beta_i\\ \delta\theta_i\end{bmatrix} = \begin{bmatrix}\delta\alpha_i^{cle}\\ \delta\beta_i^{cle}\\ \delta\theta_i^{bkl} + \delta\theta_i^{axic}\end{bmatrix}, \tag{5.9}$$

where, $\delta\alpha_i^{cle} and\ \delta\beta_i^{cle}$, $\delta\theta_i^{bkl}$, and $\delta\theta_i^{axic}$ are the rotation errors due to clearance, backlash, and joint flexibility respectively. The Cartesian positional error ΔP_{tilt} due to joints tilting can be calculated using (5.9) and the identification Jacobean as:

$$\Delta P_{tilt} = J.\Delta E^{tilt}, \tag{5.10}$$

where, $\Delta E^{tilt} = [\delta\theta_1 \ldots . \delta\theta_5\ \ \delta\alpha_2 .. \delta\alpha_5\ \ \delta\beta_3 \ldots \delta\beta_5\ ]^T$,and the Jacobin

$$J = \begin{bmatrix}\frac{\partial P_X}{\partial\theta_1}..\frac{\partial P_X}{\partial\theta_5} & \frac{\partial P_X}{\partial\alpha_1}..\frac{\partial P_X}{\partial\alpha_5} & \frac{\partial P_X}{\partial\beta_2}..\frac{\partial P_X}{\partial\beta_5}\\ \frac{\partial P_Y}{\partial\theta_1}..\frac{\partial P_Y}{\partial\theta_5} & \frac{\partial P_Y}{\partial\alpha_1}..\frac{\partial P_Y}{\partial\alpha_5} & \frac{\partial P_Y}{\partial\beta_2}..\frac{\partial P_Y}{\partial\beta_5}\\ \frac{\partial P_Z}{\partial\theta_1}..\frac{\partial P_Z}{\partial\theta_5} & \frac{\partial P_Z}{\partial\alpha_1}..\frac{\partial P_Z}{\partial\alpha_5} & \frac{\partial P_Z}{\partial\beta_2}..\frac{\partial P_Z}{\partial\beta_5}\end{bmatrix}.$$

As this research assumes perfect link lengths, a Cartesian positional error ΔP_{geom} due to small joint twist and joint offset are calculated using the identification Jacobean as:

$$\Delta P_{geom} = J.\Delta E^{geom} \tag{5.11}$$

where,

$$\Delta E^{geom} = \left[\Delta\theta_{1}^{offset} \ldots . \Delta\theta_{5}^{offset}\ \Delta\alpha_{2}^{twist} \ldots \Delta\alpha_{5}^{twist}\ \Delta\beta_{3}^{twist} \ldots \Delta\beta_{5}^{twist}\right]^{T}.$$

While ignoring errors due to temperature, control loop, and all other factors, P_{actual} can be defined using (5.10) and (5.11) as:

$$P_{actual} = P_{theor} + \Delta P_{geom} + \Delta P_{tilt} \tag{5.12}$$

From (5.7) and (5.12), the positional error can be calculated as:

$$\Delta P = \Delta P_{geom} + \Delta P_{tilt} \tag{5.13}$$

The following section will identify the positional errors due to geometric factors ΔP_{geom} and the positional errors due to joints titling ΔP_{tilt}.

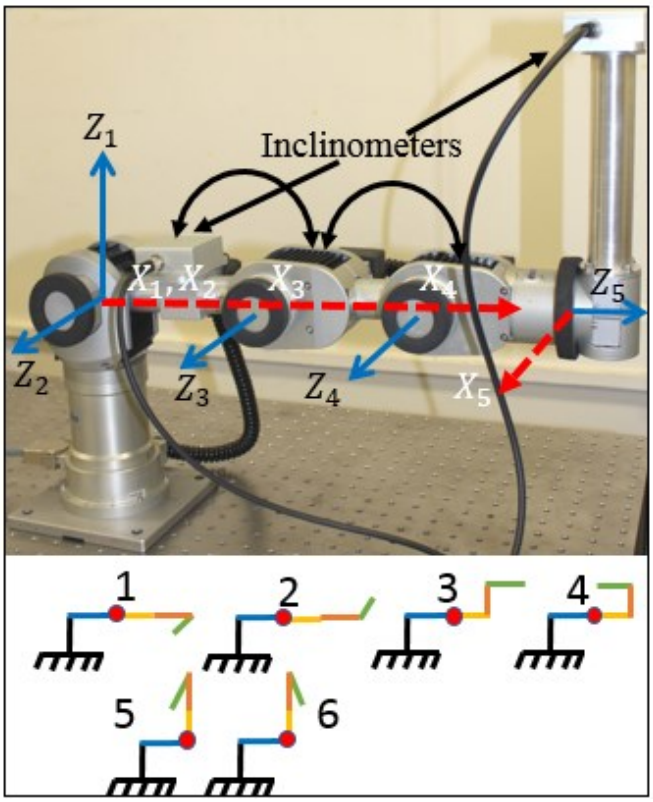

Fig. 5.4 Measurement of joint inclination, backlash and stiffness

5.3 Joint tilting modelling and error identification

Inclinometers with the resolution of 0.001° from Level Developments are used to measure various joints parameters such as joint inclination $C_i^{cle\ tilt\circ}$, backlash $\delta\theta_i^{bkl\circ}$ and joint stiffness k_i^z with the help of sufficient configurations and loading conditions such as shown in Fig. 5.4. For example, for the joint 3 highlighted in red dot, change in inclinometer's reading for configuration 1 and 2 about X-axis used to calculate $C_3^{cle\ tilt\circ}$. Relative change about Z-axis for configurations 3 and 4 gives estimation of k_3^z. A tiny shift about Z-axis between configuration 5 and 6 provides $\delta\theta_3^{bkl\circ}$. Similarly, parameters values for all joints, are obtained and listed in Table 5.2.

Table 5.2 Joints parameters

Joint i	1	2	3	4	5
$C_i^{cle\ tilt\circ}$	0.022	0.024	0.017	0.015	0.018
$\delta\theta_i^{bkl\circ}$	0.063	0.061	0.057	0.046	0.051
k_i^z (Kg-m/°)	122	90	75	78	80

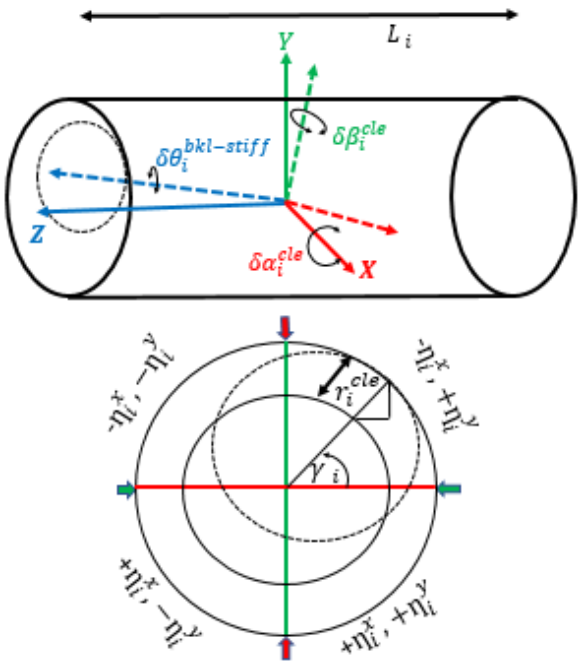

Fig. 5.5 Joint tilting model

Once the joint parameters in Table 5.2 are obtained, an instantaneous moment vector can be calculated using the recursive Newton-Euler method (Craig, 2005). If $[F_i]$ is the inertial force (considering gravitation and link acceleration), $[N_i]$ is the inertial torque, ${}_{i+1}^{i}R$ is rotational matrix from frame $\{i\}$ to frame $\{i+1\}$, $[r_i]_{i+1}$ is position vector from

frame $\{i\}$ to frame $\{i{+}1\}$, and $[s_i]_i$ is position vector from frame $\{i\}$ to center of mass of link $\{i\}$, then moment vector $[\eta_i]_i = \left[\eta_i^x\ \eta_i^y\ \eta_i^z\right]^T$ at joint $\{i\}$ can be calculated as:

$$[\eta_i]_i = [N_i] + {}_{i+1}^{i}R[\eta_{i+1}]_{i+1} + [r_i]_{i+1} \times {}_{i+1}^{i}R[f_{i+1}]_{i+1} + [s_i]_i \times [F_i]\,. \quad (5.14)$$

The value of a joint clearance r_i^{cle} in the Fig. 5.5 can be obtained from the length of a joint shaft L_i and joint inclination angle $C_i^{cle\ tilt\circ}$ from Table 5.2 as:

$$r_i^{cle} = \sqrt{\left(\frac{1}{\sin\left(C_i^{cle\ tilt}\right)^2}\right) - 1} \Big/ \left({}^{L_i}/_{2}\right) \quad (5.15)$$

Depending on the moments acting about X-axis and Y-axis, a shaft will have a single point contact inside the housing. An angle γ_i defines the contact point about the X-axis in Fig. 5.5 and can be calculated as:

$$\gamma_i = \left(\frac{|\eta_i^x| \times 1.5708}{|\eta_i^x| + |\eta_i^y|}\right) \quad (5.16)$$

Joint inclination $C_i^{cle\ tilt}$ can be resolved in two components $\delta\alpha_i$ and $\delta\beta_i$ about X-axis and Y-axis respectively as:

$$\delta\alpha_i = \frac{\eta_i^x}{|\eta_i^x|} \times \frac{r_i^{cle}\sin(\gamma_i)}{\sqrt{\left({}^{L}/_{2}\right)^2 + \left(r_i^{cle}\sin(\gamma_i)\right)^2}}, \quad (5.17)$$

$$\delta\beta_i = \frac{\eta_i^y}{|\eta_i^y|} \times \frac{r_i^{cle}\cos(\gamma_i)}{\sqrt{\left({}^{L}/_{2}\right)^2 + \left(r_i^{cle}\cos(\gamma_i)\right)^2}}. \quad (5.18)$$

Finally, $\delta\theta_i$ can be obtained by combining backlash errors and joint stiffness as:

$$\delta\theta_i = \left(\frac{\eta_i^z}{|\eta_i^z|} \times \delta\theta_i^{bkl\circ}\right) + \left({}^{\eta_i^z}/_{k_i^z}\right) \quad (5.19)$$

ΔP_{tilt} can be calculated by putting the values from (5.17), (5.18), and (5.19) in (5.10). Once ΔP_{tilt} is substituted in (5.13) any remaining positional errors can be considered as the errors due to incorrect geometric joint parameters. Geometric joint errors vector

E^{geom} can be identified iteratively (Roth et al., 1987) with the help of actual end-effector measurement for the few data points on a trajectory as:

$$E^{geom} = \frac{J^T}{J \cdot J^T} \cdot \Delta P_{geom} \tag{5.20}$$

Note that this research combines the effect of joints flexibility as the component of joints titling in (5.19). The following section will use (5.17), (5.18), and (5.19) to simulate the individual effect of joints stiffness as well as joints tilting.

5.4 Simulations

The Katana 450 robot is modelled in the MATLAB for the simulation of motion and analysis using the specifications of the robot and customised attachment used in this research. The circular Cartesian trajectory on the diagonal plane of the most significant

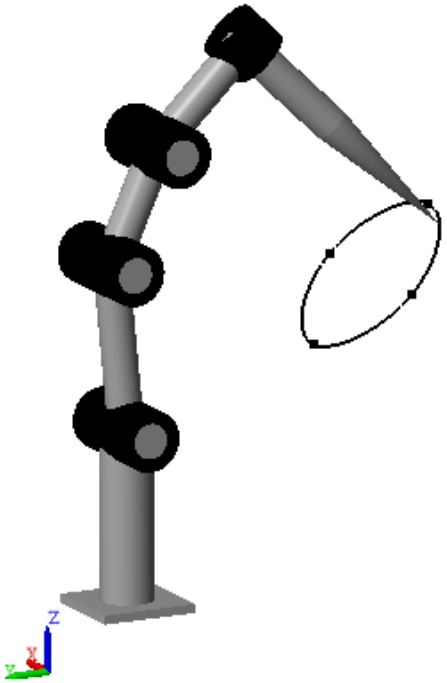

Fig. 5.6 Robot model prepared in MATLAB

frontal cube of the robot fulfils accuracy assessment criteria advised in ISO 9283 as shown in Fig. 5.6. The joint trajectories required to follow the Cartesian trajectory starting from the left-most point on the positive X-axis are shown in the Fig. 5.7.

Joints torques are obtained using joints displacement, velocities and acceleration in MATLAB which can also be obtained using (14). Calculated joints toques about Z-axis are depicted in the Fig. 5.8. Moments exerted about X-axis and Y-axis are shown

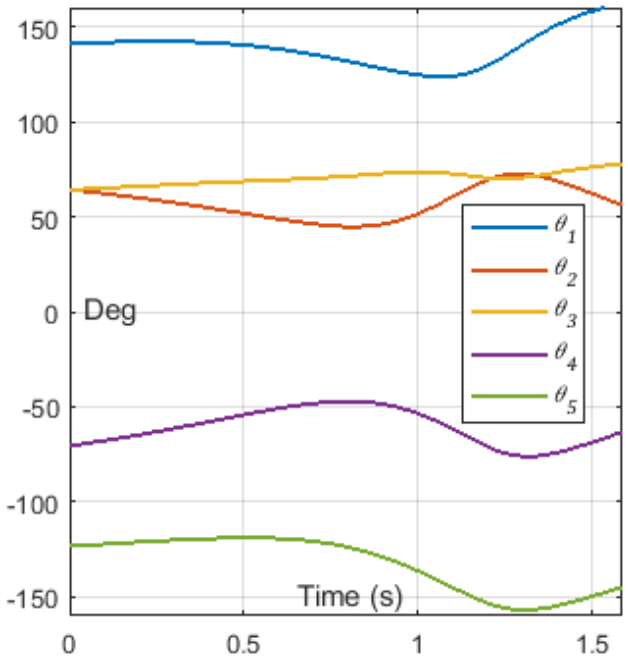

Fig. 5.7 Joint trajectories

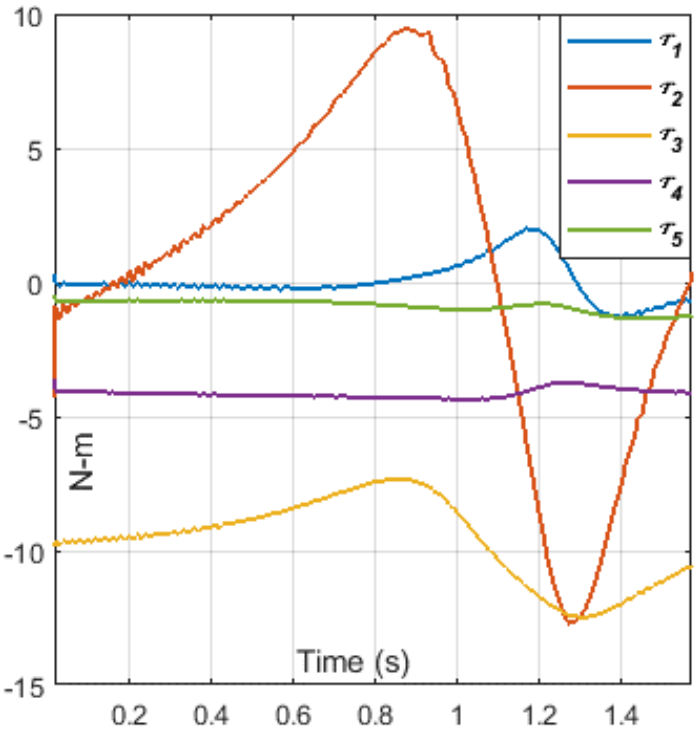

Fig. 5.8 Joint torques

in Fig. 5.9, which is supported by joint bearings. It is clear from Fig. 5.8 and Fig. 5.9 that for the vertical joint 1, the magnitude of moments about X-axis and Y-axis exceeds the actuation torque about Z-axis. Moreover, magnitude and direction of moments acting about X-axis and Y-axis for all joints change while following the trajectory. Therefore, all joints would incline (i.e. $C_i^{cle\ tilt\circ}$) based on the direction and magnitude of η_i^x and η_i^y in presence of joint clearance. Moreover, there would be a backlash error $\delta\theta_i^{bkl}$ at each joint based on direction of η_i^z, and flexibility error (i.e. η_i^z / k_i^z) depending on joint stiffness.

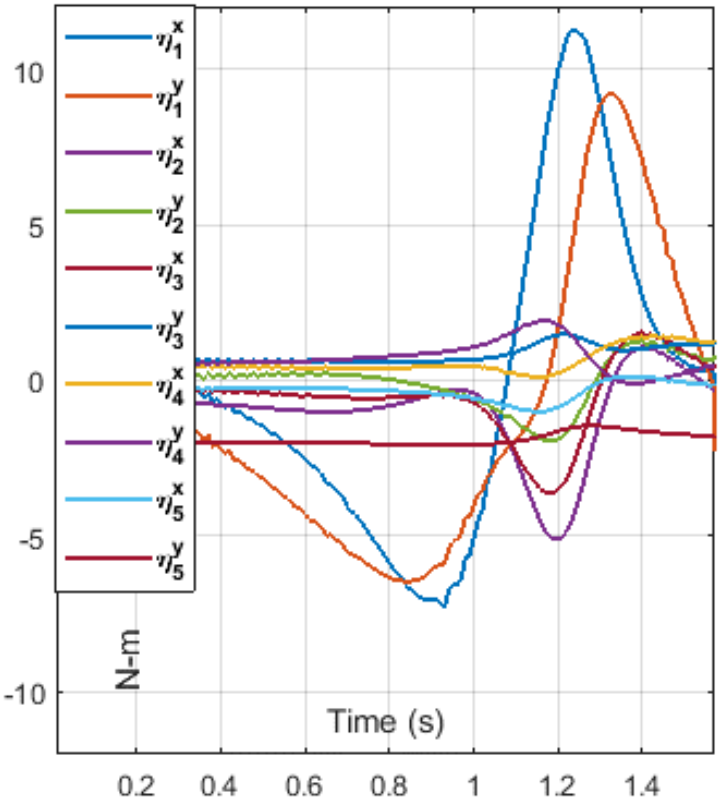

Fig. 5.9 Moments acting at joints about X and Y-axis

A perfect kinematic model of the Katana 450 robot is considered to analyse the effect of only stiffness and joint tilting. Firstly, the positional errors are calculated under the effect of joints flexibility only using the joints stiffness values from Table 5.2 in (5.19) assuming zero backlashes. The Positional errors cab be calculated as:

$$\Delta P = P_{actual} - P_{theor} = \sqrt{\Delta X^2 + \Delta Y^2 + \Delta Z^2}. \tag{5.21}$$

Next simulation run implements (5.17), (5.18) and (5.19) using all parameters from Table 5.2 to simulate the effect of joints tilting on a positional accuracy when the robot is in the motion. It is clear from the Fig. 5.10 that the joints tilting (i.e. combined effect of joint clearance, backlash and stiffness) can significantly affect the positional

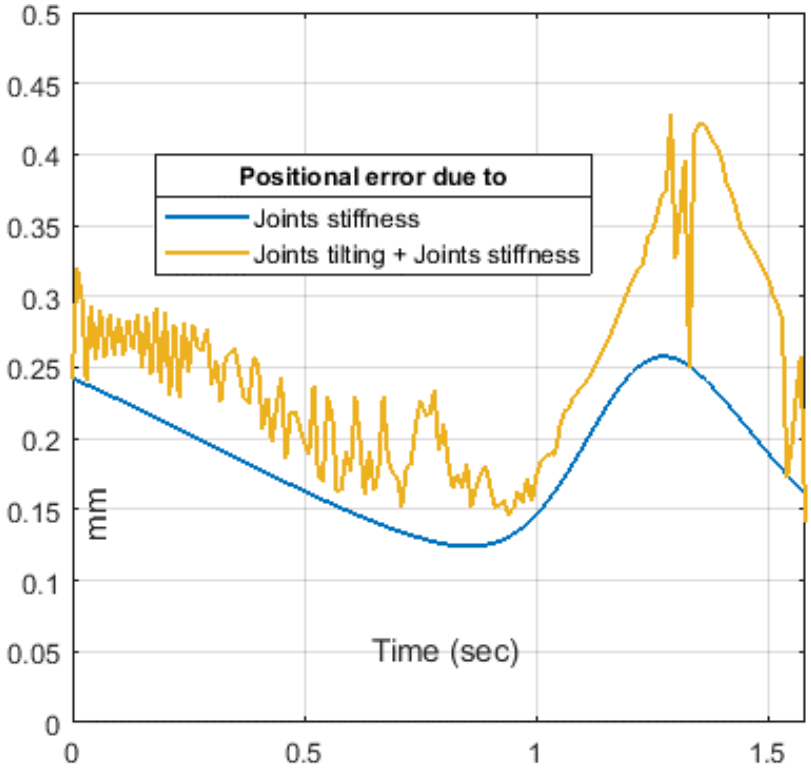

Fig. 5.10 Effect of joints stiffness and joints tilting on the positional accuracy

accuracy of the robotic manipulator. It is evident from the simulations results in Fig. 5.10 that joints tilting can significantly affect both trajectory tracking accuracy and kinematics errors identification if not ignored. The following section validates proposed approach on the Katana 450 robot with high accuracy measurement system.

5.5 Low-cost measurement setup and experiments

5.5.1 Robot calibration

NDI Optotrack system with the resolution of 0.01 mm measures the robot's end-effectors position as shown in the left-left half of Fig. 5.11. Coordinates of three active markers attached on the robot end-effector facilitate real-time position measurement at 4600 Hz. Equation (5.6) converts the end-effectors coordinates from real base to

nominal base of the robot shown in Fig. 5.11. Anti-vibration table and constant temperature in the laboratory environment provided the consistent measurements.

A circular Cartesian trajectory on a diagonal plane passing through points $[0\ -370.7107\ 210], [-100\ -300\ 139.2893], [0\ -229.2893\ 68.5786]$, and $[100\ -300\ 139.2893]$ is selected as shown in Fig. 5.6. Difference between the actual measurements using the Optotrack system P_{actual} and a desired Cartesian trajectory P_{theor} gives positional errors ΔP before calibration as shown in Fig. 5.12. Firstly, errors due to joints tilting are incorporated (i.e. using (5.6), (5.10), and (5.17-5.19)) as

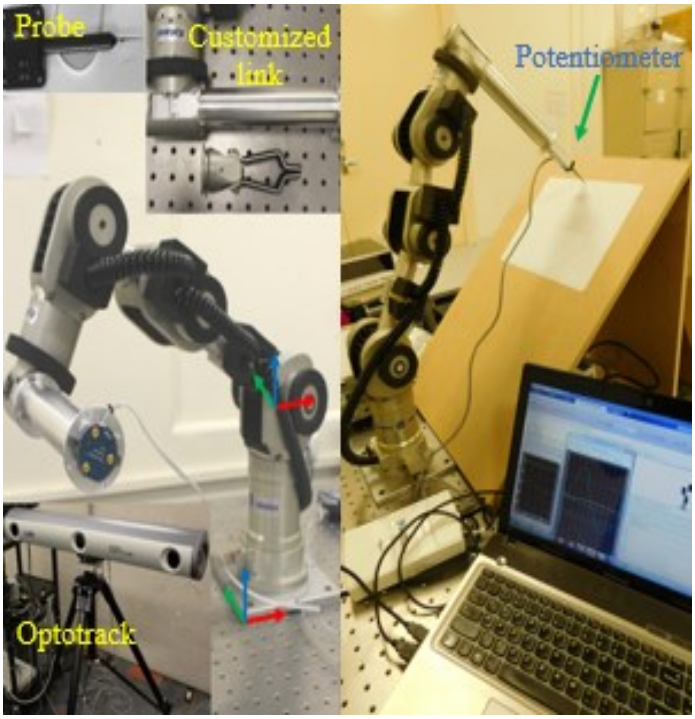

Fig. 5.11 Experimental set-up

like the one in Fig. 5.10 to obtain a new trajectory $P_{tilting}$. The newly estimated Cartesian trajectory $P_{tilting}$ considering joints tilting and actual Cartesian trajectory P_{actual} had the narrower positional difference. Secondly, the newly estimated Cartesian trajectory $P_{tilting}$ is discretised to obtain few samples of positional errors ΔPs by comparing against actual measurements P_{actual}. The positional error ΔP over these data points are assumed to be an error due to geometric factors (i.e. ΔP_{geom} in (5.20)), and used to correct geometric joints parameters (i.e. $\Delta\theta_i^{offset}, \Delta\alpha_i^{twist}, and\ \Delta\beta_i^{twist}$). Finally, consideration of the joints tilting, and correction of geometric errors together leads to a Cartesian trajectory $P_{tilting-geom}$

which is the closer representation of an actual behavior of a robot (i.e. (5.12)). However, to achieve the desired trajectory P_{theor}, joint trajectories must be modified according to the difference between estimated trajectory $P_{tilting-geom}$ and calculated trajectory P_{theor} to obtain final Cartesian trajectory P_{final} as:

$$\Delta\theta^{correction} = \frac{J^T}{J \cdot J^T} \cdot (P_{tilting-geom} - P_{theor}), \tag{5.22}$$

where, $\Delta\theta^{correction} = [\delta\theta_1\ \delta\theta_2\ \delta\theta_3\ \delta\theta_4\ \delta\theta_5\ ]^T$,and the Jacobin $J = \begin{bmatrix} \frac{\partial P_X}{\partial \theta_1} \cdots \frac{\partial P_X}{\partial \theta_5} \\ \frac{\partial P_Y}{\partial \theta_1} \cdots \frac{\partial P_Y}{\partial \theta_5} \\ \frac{\partial P_Z}{\partial \theta_1} \cdots \frac{\partial P_Z}{\partial \theta_5} \end{bmatrix}$.

Fig. 5.12 shows an error between the final trajectory P_{final} and P_{actual} after the calibration. Even though, there are more substantial positional errors (i.e. blue line in

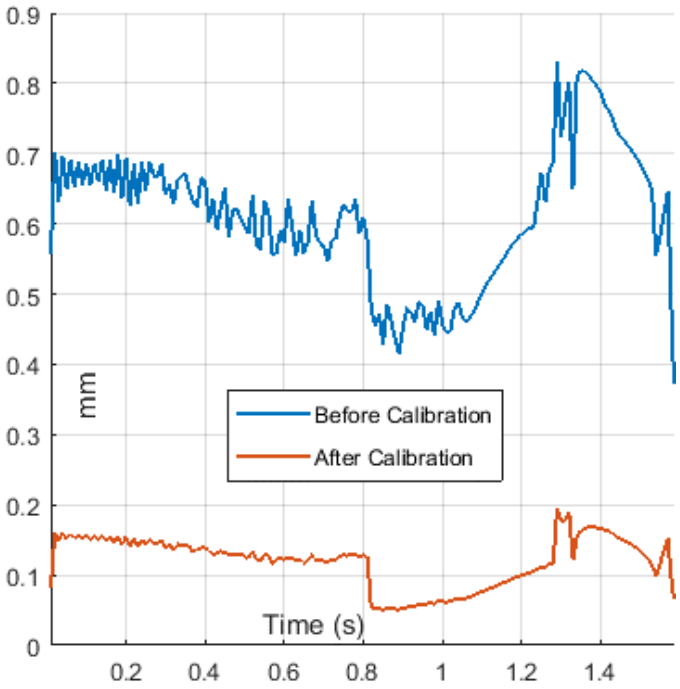

Fig. 5.12 Positional errors measured using
NDI Optotrack before and after the calibration

Fig. 5.12) compare to the simulations (yellow line in Fig. 5.10), the trend of error is similar, which indicates the effect of joints tilting. The trend of error is not the same because inaccuracy of geometric joint parameters has the configuration dependent influence on the positional errors as explained in Fig. 5.1. If robot would have only

link length errors (i.e. zero joint twist and joint offset error), then the simulated error plot in Fig. 5.10 would be just shifted towards higher value for the actual measurement in Fig. 5.12. Note that proposed calibration method first calculates joints tilting (i.e. due to clearance, backlash and stiffness) before correcting geometric joints parameters error (i.e. $\Delta\theta_i^{offset}, \Delta\alpha_i^{twist}, and\ \Delta\beta_i^{twist}$). Geometric errors remain consistent over the entire workspace of the robot. Therefore, geometric parameters need not to be corrected for a different trajectory once calibrated. Moreover, Equation (5.22) doesn't require the data of actual measurements as it is the correction between desired trajectory P_{theor} and estimated trajectory $P_{tilting-geom}$. The last step (i.e. (5.22)) can be avoided if the trajectory is planned with the corrected kinematics parameters and incorporating joints tilting (i.e. using $P_{tilting-geom}$).

The current geometric error identification solely reduced average errors from 0.653 to 0.312 mm. Moreover, consideration of pose errors due to joints stiffness before standard kinematics error identification reduces error from 0.653 to 0.211 mm. The average positional error over the circular Cartesian trajectory drops down from 0.653 mm to 0.132 mm after implementation of proposed calibration approach which is the significant reduction in positional errors compare to previously proposed calibration approaches. The robot followed a straight line profile with an average accuracy of 0.151 mm in the separate experiment which indicates a consistency of improved accuracy over the entire robot workspace.

5.5.2 Low-cost set-up for validation

Because positional measurements are sufficient to assess the accuracy of a robot (Klimchik et al., 2013), this research proposes a low-cost set-up to validate the improvement in the tracking accuracy after the calibration instead of a costly measurement equipment used for the research. The proposed set-up is partially inspired by the previously suggested low-cost measurement technique using LVDT and inclinometers (Karlsson and Brogårdh, 2001). The inclinometers nowadays can accurately measure an angular deviation with a precision of thousandth part of a degree in a static condition and can be used to obtain parameters in Table 2. However, it is not possible to measure with the same accuracy in the dynamic condition (i.e. when the robot is in the motion). Therefore, this research proposes an inexpensive method using pencil, paper, plane and potentiometer as shown in the right half of Fig. 5.11.

The robot is manually moved to four distinct points which are quarter apart on a printed circle on a diagonal plane at 45° to acquire a 3D circular trajectory in a Cartesian space shown in the top-right corner of Fig. 5.6. A pencil is attached to a potentiometer with a spring in between, which is fixed on the robot end-effector to measure the error in the Z-direction of a robot tool shown in the right half of Fig. 5.11. The potentiometer gives a signal for any deviation in a +Z/-Z direction to the MATLAB through the Data Acquisition Card (DAQ) as shown in the bottom-right of Fig. 5.13. Note that the purpose of the presented measurement set-up is to validate the improvement in the accuracy. The set-up can be used to estimate Cartesian positional errors over few data points with the help of a relative change in joint angles required to manually move between few selected points on the circle from the actual position

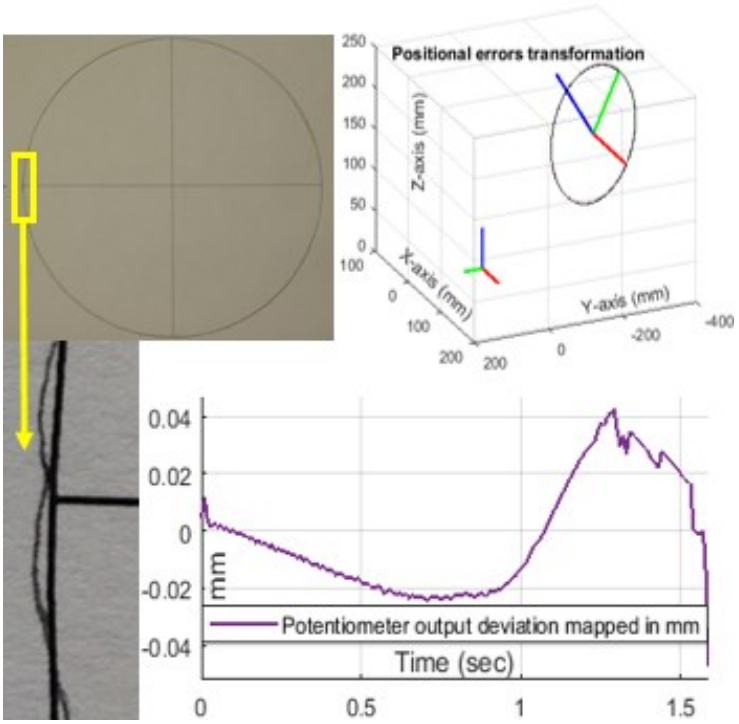

Fig. 5.13 Low-cost measurement outcome

and potentiometers output (Ha, 2008). Image processing can be used in conjunction with the potentiometer output to directly measure Cartesian errors instead of approximating from the relative change in the joint angles.

The output of potentiometer (+/-Z-direction) and a profile plotted (XY- direction) on a paper by the robot combinedly provide Cartesian errors concerning a coordinate system at the centre of a circular profile shown in the top-right corner of Fig. 5.13. Equations (15-20) can be used for robot calibration as explained in Section 5.1.

Proposed set-up can be used to visually recognise an improvement in trajectory tracking accuracy before and after the calibration.

5.6 Conclusion

Joint clearance, backlash, and stiffness of a robotic joint can harshly affect the tracking accuracy of serial robotic manipulators and can be combinedly addressed as a joint tilting. The standard kinematics errors identification may be incorrect if joints tilting is not compensated beforehand. Joint tilting errors must be considered to achieve dynamic accuracy below 0.1 mm over entire workspace of a serial robot. The proposed calibration approach can be readily used for the trajectory planning in the application such as a robotic laser cutting and welding. However, further investigation would be required for the case where robot's end-effector is subject to external loading conditions for the applications such as robotic welding.

Acknowledgement

We would like to thank the School of Mechanical Engineering, the University of Adelaide for providing resources and assistance in for the research.

CHAPTER 6 CONCLUSION AND FUTURE WORK

6.1 Conclusion

Literature focused on the serial robot calibration suggested that none of the previous research has considered the configuration dependent effect of joint kinematics parameters on the pose accuracy of a serial robot during the errors identification. This research has not only analyzed influence of kinematics parameters over the entire robot workspace, but also recommended influence-based errors identification. This research has proved that influence based geometric errors identification is effective than the conventional errors identification. This research also establishes the fact that joints tilting because of clearance, backlash and stiffness can significantly affect the accuracy of a serial robotic manipulator. Estimation of possible pose errors due to joints tilting before conventional geometric error identification can improve pose accuracy over entire workspace. The overall results in this research indicates that only kinematics errors identification can improve the average accuracy of a robot up to 50 % over entire workspace. Consideration of joints stiffness along with the kinematics errors identification can increase accuracy up to 68 %. The proposed approach of considering the joints tilting during the robot calibration can improve the accuracy up to 80% over entire workspace of a robot which is the significant improvement in the accuracy.

6.2 Future work

Still, there is scope to combine influence-based errors identification and joint tilting model to further improve trajectory tracking accuracy. One can follow the methodology described in Chapter 5, where geometric errors identification in (5.20) needs to follow the method suggested in Chapter 3. Moreover, joints tilting model can be enhanced to estimate the pose errors when robot end-effector is subjected to external loading. Besides, the effectiveness of the proposed low-cost measurement set-up in validating the improvements in accuracy after the calibration, further research would be required to measure positional errors using image processing. The potentiometer and pencil can be replaced with LVDT and double ball bar respectively for more accurate measurements. The joint tilting may affect the joint encoder's reading (Li and Fan, 2017), and would also require further investigation.

REFERENCES

ANGELIDIS, A. & VOSNIAKOS, G.-C. 2014. Prediction and compensation of relative position error along industrial robot end-effector paths. *International journal of precision engineering and manufacturing,* 15**,** 63-73.

CAENEN, J. L. & ANGUE, J. C. 1990. Identification of geometric and nongeometric parameters of robots. 1032-1037.

CANTELLI, L., MUSCATO, G., NUNNARI, M. & SPINA, D. 2015. A Joint-Angle Estimation Method for Industrial Manipulators Using Inertial Sensors. *IEEE/ASME Transactions on Mechatronics,* 20**,** 2486-2495.

CHEN-GANG, C., TONG, L., MING, C., QING, J. & XU, S. 2014. Review on Kinematics Calibration Technology of Serial Robots, Int. *Journal of Precision Engineering and Manufacturing,* 15**,** 1759-1774.

CRAIG, J. J. 1990. *Introduction to Robotics: Mechanics and Control*, Addison-Wesley.

CRAIG, J. J. 2005. *Introduction to robotics: mechanics and control*, Pearson Prentice Hall Upper Saddle River.

DU, G. & ZHANG, P. 2013. IMU-based online kinematic calibration of robot manipulator. *The Scientific World Journal,* 2013.

DUMAS, C., CARO, S., GARNIER, S. & FURET, B. 2011. Joint stiffness identification of six-revolute industrial serial robots. *Robotics and Computer-Integrated Manufacturing,* 27**,** 881-888.

GE, J., GU, H., LU, Q. & LI, Q. An Automatic Industrial Robot Cell Calibration Method. ISR/Robotik 2014; 41st International Symposium on Robotics, 2-3 June 2014 2014. 1-6.

GONG, C., YUAN, J. & NI, J. 2000. Nongeometric error identification and compensation for robotic system by inverse calibration. *International Journal of Machine Tools and Manufacture,* 40**,** 2119-2137.

HA, I.-C. 2008. Kinematic parameter calibration method for industrial robot manipulator using the relative position. *Journal of Mechanical Science and Technology,* 22**,** 1084-1090.

HAYATI, S. & MIRMIRANI, M. 1985. Improving the absolute positioning accuracy of robot manipulators. *Journal of Field Robotics,* 2**,** 397-413.

HEPING, C., FUHLBRIGGE, T., SANG, C., JIANJUN, W. & XIONGZI, L. Practical industrial robot zero offset calibration. 2008 IEEE International Conference on Automation Science and Engineering, 23-26 Aug. 2008 2008. 516-521.

JANG, J. H., KIM, S. H. & KWAK, Y. K. 2001. Calibration of geometric and non-geometric errors of an industrial robot. *Robotica,* 19**,** 311-321.

JAWALE, H. & THORAT, H. 2013. Positional error estimation in serial link manipulator under joint clearances and backlash. *Journal of Mechanisms and Robotics,* 5**,** 021003.

JOHNSRUD, V. 2014. *Improvement of the Positioning Accuracy of Industrial Robots.* Mechanical Engineering Masters, Norwegian University of Science and Technology.

JOUBAIR, A. & BONEV, I. A. 2015. Non-kinematic calibration of a six-axis serial robot using planar constraints. *Precision Engineering,* 40**,** 325-333.

KAKIZAKI, T., DECK, J. F. & DUBOWSKY, S. 1993. Modeling the Spatial Dynamics of Robotic Manipulators with Flexible Links and Joint Clearances. *Journal of Mechanical Design,* 115**,** 839-847.

KARLSSON, B. & BROGÅRDH, T. 2001. A new calibration method for industrial robots. *Robotica,* 19.

KHALIL, W. & BESNARD, S. 2002. Geometric calibration of robots with flexible joints and links. *Journal of Intelligent & Robotic Systems,* 34**,** 357-379.

KLIMCHIK, A., CARO, S., WU, Y., FURET, B. & PASHKEVICH, A. Advanced robot calibration using partial pose measurements. 2013 18th International Conference on Methods & Models in Automation & Robotics (MMAR), 26-29 Aug. 2013 2013. 264-269.

KLIMCHIK, A., WU, Y., DUMAS, C., CARO, S., FURET, B. & PASHKEVICH, A. Identification of geometrical and elastostatic parameters of heavy industrial robots. Robotics and Automation (ICRA), 2013 IEEE International Conference on, 2013. IEEE, 3707-3714.

LI, Y.-T. & FAN, K.-C. 2017. A novel method of angular positioning error analysis of rotary stages based on the Abbe principle. *Proceedings of the Institution of Mechanical Engineers, Part B: Journal of Engineering Manufacture***,** 095440541668893.

LIU, Y., XI, N., ZHANG, G., LI, X., CHEN, H., ZHANG, C., JEFFERY, M. J. & FUHLBRIGGE, T. A. An automated method to calibrate industrial robot joint offset using virtual line-based single-point constraint approach. 2009 IEEE/RSJ International Conference on Intelligent Robots and Systems, 10-15 Oct. 2009 2009. 715-720.

MEGGIOLARO, M. A. & DUBOWSKY, S. 2000. An analytical method to eliminate the redundant parameters in robot calibration. 4**,** 3609-3615.

MENG, Y. & ZHUANG, H. 2007. Autonomous robot calibration using vision technology. *Robotics and Computer-Integrated Manufacturing,* 23**,** 436-446.

MOORING, B. W., ROTH, Z. S. & DRIELS, M. R. 1991. *Fundamentals of manipulator calibration*, Wiley New York.

NUBIOLA, A. & BONEV, I. A. 2013. Absolute calibration of an ABB IRB 1600 robot using a laser tracker. *Robotics and Computer-Integrated Manufacturing,* 29**,** 236-245.

NUBIOLA, A., SLAMANI, M. & BONEV, I. A. 2013. A new method for measuring a large set of poses with a single telescoping ballbar. *Precision Engineering,* 37**,** 451-460.

NUBIOLA, A., SLAMANI, M., JOUBAIR, A. & BONEV, I. A. 2013. Comparison of two calibration methods for a small industrial robot based on an optical CMM and a laser tracker. *Robotica,* 32**,** 447-466.

PARK, F. C. & OKAMURA, K. 1994. Kinematic Calibration and the Product of Exponentials Formula. 119-128.

PARK, I.-W. & KIM, J.-H. Estimating entire geometric parameter errors of manipulator arm using laser module and stationary camera. IECON 2011-37th Annual Conference on IEEE Industrial Electronics Society, 2011. IEEE, 129-134.

PATEL, D., LU, T.-F. & CHEN, L. 2017. An Influence Based Error Identification for Kinematics Calibration of Serial Robotic Manipulators. *5th IFToMM International Symposium on Robotics & Mechatronics (ISRM2017).* Sydney, Australia.

RENDERS, J. M., ROSSIGNOL, E., BECQUET, M. & HANUS, R. 1991. Kinematic calibration and geometrical parameter identification for robots. *IEEE Transactions on Robotics and Automation,* 7**,** 721-732.

ROTH, Z., MOORING, B. & RAVANI, B. 1987. An overview of robot calibration. *IEEE Journal on Robotics and Automation,* 3**,** 377-385.

SANTOLARIA, J. & GINÉS, M. 2013. Uncertainty estimation in robot kinematic calibration. *Robotics and Computer-Integrated Manufacturing,* 29**,** 370-384.

SHIAKOLAS, P., CONRAD, K. & YIH, T. 2002. On the accuracy, repeatability, and degree of influence of kinematics parameters for industrial robots. *International journal of modelling and simulation,* 22**,** 245-254.

ŠVACO, M., ŠEKORANJA, B., ŠULIGOJ, F. & JERBIĆ, B. 2014. Calibration of an Industrial Robot Using a Stereo Vision System. *Procedia Engineering,* 69**,** 459-463.

TAO, P. Y., YANG, G., SUN, Y. C., TOMIZUKA, M. & LAI, C. Y. 2012. Product-of-exponential (POE) model for kinematic calibration of robots with joint compliance. 496-501.

TIAN, W., MEI, D., LI, P., ZENG, Y., HONG, P. & ZHOU, W. 2015. Determination of optimal samples for robot calibration based on error similarity. *Chinese Journal of Aeronautics,* 28**,** 946-953.

TO, M. H. 2012. A framework for flexible integration in robotics and its applications for calibration and error compensation.

WANG, C., CHEN, W. & TOMIZUKA, M. Robot end-effector sensing with position sensitive detector and inertial sensors. 2012 IEEE International Conference on Robotics and Automation, 14-18 May 2012 2012. 5252-5257.

WU, Y., KLIMCHIK, A., CARO, S., FURET, B. & PASHKEVICH, A. 2015. Geometric calibration of industrial robots using enhanced partial pose measurements and design of experiments. *Robotics and Computer-Integrated Manufacturing,* 35**,** 151-168.

XIAO-LIN, Z. & LEWIS, J. M. 1995. A new method for autonomous robot calibration. *Proceedings of 1995 IEEE International Conference on Robotics and Automation.*

ZHAO, Y. M., LIN, Y., XI, F. & GUO, S. 2015. Calibration-Based Iterative Learning Control for Path Tracking of Industrial Robots. *IEEE Transactions on Industrial Electronics,* 62**,** 2921-2929.

ZHOU, J., NGUYEN, H.-N. & KANG, H.-J. 2014. Simultaneous identification of joint compliance and kinematic parameters of industrial robots. *International journal of precision engineering and manufacturing,* 15**,** 2257-2264.

ZHU, J. & TING, K.-L. 2000. Uncertainty analysis of planar and spatial robots with joint clearances. *Mechanism and Machine Theory,* 35**,** 1239-1256.

ZHUANG, H., ROTH, Z. S. & HAMANO, F. A complete and parametrically continuous kinematic model for robot manipulators. Robotics and Automation, 1990. Proceedings., 1990 IEEE International Conference on, 1990. IEEE, 92-97.

ZHUANG, H., WANG, L. K. & ROTH, Z. S. 1993. Error-model-based robot calibration using a modified CPC model. *Robotics and computer-integrated manufacturing,* 10**,** 287-299.